FINITE-AMPLITUDE STANDING WAVES IN REAL CAVITIES CONTAINING DEGENERATE MODES

Winfield Scott Slocum

NAVAL POSTGRADUATE SCHOOL
Monterey, California

THESIS

FINITE-AMPLITUDE STANDING WAVES IN REAL CAVITIES CONTAINING DEGENERATE MODES

by

Winfield Scott Slocum IV

December 1975

Thesis Advisor: James V. Sanders

Approved for public release; distribution unlimited.

SECURITY CLASSIFICATION OF THIS PAGE (*When Data Entered*)

REPORT DOCUMENTATION PAGE		READ INSTRUCTIONS BEFORE COMPLETING FORM
1. REPORT NUMBER	2. GOVT ACCESSION NO.	3. RECIPIENT'S CATALOG NUMBER
4. TITLE (*and Subtitle*) Finite-Amplitude Standing Waves in Real Cavities Containing Degenerate Modes		5. TYPE OF REPORT & PERIOD COVERED Master's Thesis December 1975
		6. PERFORMING ORG. REPORT NUMBER
7. AUTHOR(*s*) Winfield Scott Slocum IV		8. CONTRACT OR GRANT NUMBER(*s*)
9. PERFORMING ORGANIZATION NAME AND ADDRESS Naval Postgraduate School Monterey, California 93940		10. PROGRAM ELEMENT, PROJECT, TASK AREA & WORK UNIT NUMBERS
11. CONTROLLING OFFICE NAME AND ADDRESS Naval Postgraduate School Monterey, California 93940		12. REPORT DATE December 1975
		13. NUMBER OF PAGES 63
14. MONITORING AGENCY NAME & ADDRESS(*if different from Controlling Office*) Naval Postgraduate School Monterey, California 93940		15. SECURITY CLASS. (*of this report*) Unclassified
		15a. DECLASSIFICATION/DOWNGRADING SCHEDULE

16. DISTRIBUTION STATEMENT (*of this Report*)

Approved for public release; distribution unlimited.

17. DISTRIBUTION STATEMENT (*of the abstract entered in Block 20, if different from Report*)

18. SUPPLEMENTARY NOTES

19. KEY WORDS (*Continue on reverse side if necessary and identify by block number*)

20. ABSTRACT (*Continue on reverse side if necessary and identify by block number*)

Finite-amplitude standing waves in air at ambient temperatures contained within a rigid-walled rectangular cavity having one variable interior dimension were experimentally investigated. The effect of degenerate or nearly degenerate configurations on the harmonic content of the observed pressure waveform was compared to the theory of Coppens and Sanders as modified to include empirically determined losses and resonances. Second and third

DD FORM 1 JAN 73 1473 EDITION OF 1 NOV 65 IS OBSOLETE
(Page 1) S/N 0102-014-6601 |

SECURITY CLASSIFICATION OF THIS PAGE (*When Data Entered*)

harmonic distortion for both degenerate and nondegenerate cavity configurations were recorded as continuous functions of frequency in the vicinity of the resonances for the 100 and 110 modes. It was found that in rectangular cavities having walls free of any perturbation, the theoretical model can accurately predict both shapes and amplitudes of the harmonic content of the finite-amplitude standing wave whether or not degeneracies are present.

Finite-Amplitude Standing Waves
in
Real Cavities Containing Degenerate Modes

by

Winfield Scott Slocum IV
Lieutenant, United States Navy
B.S., Ohio State University, 1969

Submitted in partial fulfillment of the
requirements for the degree of

MASTER OF SCIENCE IN ENGINEERING ACOUSTICS

from the

NAVAL POSTGRADUATE SCHOOL
December 1975

ABSTRACT

Finite-amplitude standing waves in air at ambient temperatures contained within a rigid-walled rectangular cavity having one variable interior dimension were experimentally investigated. The effect of degenerate or nearly degenerate configurations on the harmonic content of the observed pressure waveform was compared to the theory of Coppens and Sanders as modified to include empirically determined losses and resonances. Second and third harmonic distortion for both degenerate and nondegenerate cavity configurations were recorded as continuous functions of frequency in the vicinity of the resonances for the 100 and 110 modes. It was found that in rectangular cavities having walls free of any perturbation, the theoretical model can accurately predict both shapes and amplitudes of the harmonic content of the finite-amplitude standing wave whether or not degeneracies are present.

TABLE OF CONTENTS

LIST OF TABLES

LIST OF ILLUSTRATIONS

ACKNOWLEDGEMENTS

The generous aid and encouragement of Professors James V. Sanders and Alan B. Coppens is gratefully acknowledged.

Sincere thanks and appreciation are also due to Mr. Robert C. Moeller for his exceptional assistance in fabricating parts of the experimental setup.

Thanks should also be extended to Ensign John Jay Donnelly for his assistance and general companionship during the many hours spent in data collection.

Appreciation to the U. S. Naval Postgraduate School Research Foundation for purchasing the Automatic Level Regulator is willingly acknowledged.

I. INTRODUCTION

In 1968, Coppens and Sanders [1] applied a one-dimensional, nonlinear, acoustic wave equation with a dissipative term describing absorptive losses to rigid-walled, closed tubes with large length-to-diameter ratios. They later expanded this theory to incorporate empirically determined losses and resonance frequencies [2]. The model was further extended to include two- and three-dimensional cases, which was experimentally investigated by Lane [3] and Devall [4].

One of the significant results of these latter investigations was that the agreement between theory and experiment deteriorated when degenerate modes were present. The theory was not able to account for the effect of modes degenerate to members of the family of the driven mode.

To study the effects of degeneracies, a rectangular cavity was designed and constructed so that one wall could be moved and secured at various positions to introduce or remove degenerate modes as desired. The primary interest in this research is to make a detailed investigation of finite-amplitude standing waves in air at ambient temperatures in cavity configurations producing degenerate or nearly degenerate modes, and compare the results to the present state of the theory of Coppens and Sanders.

II. BACKGROUND AND THEORY

The study of distortion of intense acoustic waves began in 1868 when Kirchoff [5] used the nonviscous hydrodynamic equations to predict a change in waveform for a plane traveling longitudinal wave. The investigations of finite amplitude effects in traveling waves continued [6,7,8], and in 1954 Keller [9] was able to extract solutions for standing waves in a closed tube. His investigations, based on a nondissipative medium, yielded useful results for frequencies away from resonance, but predicted infinite amplitudes at resonance.

In absorptive media, only those waves of relatively high amplitude will experience a change in form. The solution of this nonlinear wave equation requires second order terms or higher, which Keck and Beyer [10] developed using perturbation methods and Fourier series representation of the waveform. Coppens and Sanders [1] extended the perturbation approach to include wall losses predicted by Rayleigh-Kirchoff [11], and showed excellent agreement with experiments conducted in a rigid-walled tube at low levels of nonlinear interactions. The experimental work by Beech [12] with supporting calculation by Ruff [13] showed that at high excitation levels, a significant difference developed between theory and experiment. Winn [14] experimentally demonstrated

that the Rayleigh-Kirchoff loss mechanisms were not completely suitable in describing the phase relationships observed in the distorted waveform. Coppens and Sanders [3] then revised their model to utilize empirically determined losses and resonant frequencies, thereby extending the excellent agreement between theory and experiment to higher excitation levels. A further extension of their model to two- and three-dimensional standing waves in cavities was purposed and experimentally found by Lane [3], to successfully predict the major features of the harmonic content for finite-amplitude standing waves in rectangular cavities. Devall [4], however, found that if degeneracies existed, the model failed to account for the experimentally observed excitation of non-family modes.

The model of Coppens and Sanders is based on a three-dimensional, nonlinear wave equation with a dissipative term describing absorptive losses encountered by plane standing waves in rigid walled cavities. In one dimension, the wave equation takes the form

$$\sum_{n=1}^{\infty} \left(\frac{\partial^2}{\partial x^2} - \frac{1}{C_o^{\,2}} \frac{\partial^2}{\partial t^2} + D_n\right) \frac{\partial \zeta_n}{\partial x} = b \frac{\partial^2}{\partial x^2} \left(\frac{\partial \zeta}{\partial x}\right)^2 \qquad (1)$$

where

ζ_n = particle displacement due to n^{th} harmonic

$\zeta = \sum_n \zeta_n$

$b = 1/2(1 + C_p/C_v)$

C_p = specific heat for medium at constant pressure

C_v = specific heat for medium at constant volume.

The term D_n depends on the loss mechanism, and for Rayleigh-Kirchoff wall losses is

$$D_n = \delta_1 \left(\frac{1}{(\omega_{1r}) n^{3/2}} \frac{\partial^3}{\partial x^2 \partial t} - \frac{1}{n^{1/2}} \frac{\partial^2}{\partial x^2} \right)$$

where

δ_1 = a coefficient containing the shear viscosity and thermal conductivity of the medium

ω_{1r} = frequency (angular) of fundamental resonance

$Q_1 = \dfrac{\omega_{1r}}{\omega_{1+} - \omega_{1-}}$

and $\omega_{1+} - \omega_{1-}$ is the difference of the half power frequencies above and below the fundamental.

Equation 1 can be reformulated [3] to introduce the empirical resonance frequencies and absorption coefficients. This results in

$$\sum_{n=1}^{\infty} K_n^2 \left[\frac{2\Delta\omega_n}{\omega_{nr}} - \frac{1}{n\omega} \frac{1}{Q_n} \frac{\partial}{\partial t} \right] \frac{\partial \zeta_n}{\partial x} = b \frac{\partial^2}{\partial x^2} \left(\frac{\partial \zeta}{\partial x} \right)^2 \qquad (2)$$

where

$K_n = \dfrac{4\pi}{nL}$

ω_{nr} = resonance frequency of the n^{th} overtone

$\Delta\omega_n = n\omega - \omega_{nr}$

ω = driving frequency (near ω_{1r})

$Q_n = \dfrac{\omega_{nr}}{\omega_{n+} - \omega_{n-}}$

($\omega_{n+} - \omega_{n-}$ is the difference of the half power frequencies above and below ω_{nr}.)

$$\frac{\partial\zeta}{\partial x} = \frac{p}{\rho_o C_o^2} = M \sum_{n=1}^{\infty} R_n \cos K_n(L-X) \cos n(\omega t + \phi_n)$$

p = acoustic pressure

ρ_o = density of medium

C_o = thermodynamic speed of sound in medium

M = mach number = $P_1/\rho_o C_o^2$

P_1 = peak pressure of fundamental component of wave

R_n = Fourier coefficient of n^{th} harmonic component, normalized such that $R_1 = 1$

and

ϕ_n = phase angle of n^{th} harmonic component, where $\phi_1 = 0$.

Equation 2 can be changed into a time-independent form, which when solved for boundary conditions of rigid walls produces

$$H_n R_n \cos(\phi_n - \theta_n) = MbQ_1 \frac{1}{2} \left\{ \frac{1}{2} \sum_{j=1}^{n=1} R_j R_{n-j} \cos(\phi_j + \phi_{n-j}) - \sum_{j=1}^{\infty} R_{n+j} R_j \cos(\phi_{n+j} - \phi_j) \right\}$$

and a similar form with sin in place of cos, where

$$H_n = \left\{ \left(\frac{2\Delta\omega_n}{\omega_{nr}} Q_1\right)^2 + \left(\frac{Q_1}{Q_n}\right)^2 \right\}^{1/2}$$

and

$$\tan\theta_n = \frac{2\Delta\omega_n Q_1/\omega_{nr}}{Q_1/Q_n}$$

A quantity E(n) is defined

$$E(n) = \frac{\omega_{nr} - n\omega_{1r}}{n\omega_{1r}}$$

to indicate the position of ω_{nr} relative to the ideal harmonic frequencies, $n\omega_{1r}$. Values for Q(n) and E(n) are directly determined from infinitesimal-amplitude analysis of the cavity, and are used as computer input parameters.

III. EXPERIMENTAL CONSIDERATIONS

A. APPARATUS

The rectangular cavity used in this research (Figure 1) was constructed from 0.982 in. milled aluminum plates. The interior of the cavity was 12.002 in. long and 2.502 in. high, while the width could be varied from approximately 5.50 in. to 7.00 in. in 0.25 in. increments. All joints were right angles, to which a thin layer of silicon grease was applied prior to assembly to hermetically seal the cavity. Table I shows the theoretically predicted normal mode frequencies for ideal rectangular cavities corresponding to the seven nominal configurations.

Acoustic waves were introduced into the cavity by means of a piston located in a 2.25 in. diameter port in the floor. A single lubricated O-ring was used to produce a seal between the piston and the port.

On a side wall opposite the piston, another port was cut for a 1/4 in. diameter Bruel and Kjaer type 4136 condenser microphone. This port contained two small O-rings to provide a seal for the microphone. The axes of the piston and microphone were mutually perpendicular to minimize coupling of mechanical vibration.

A block diagram of the apparatus is shown in Figure 2. The piston was driven by an M-B Electronics Model EA1500

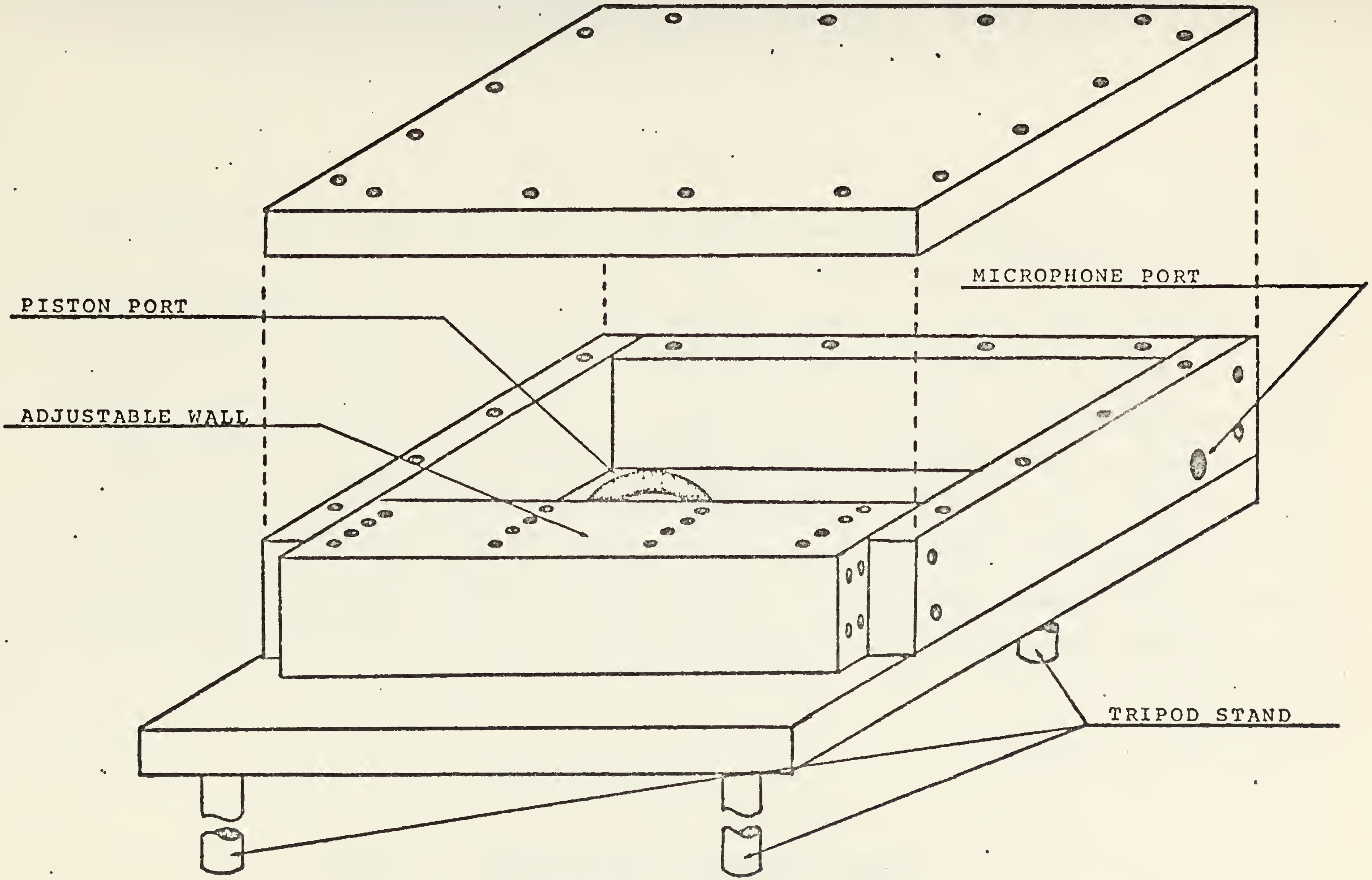

FIGURE 1. ADJUSTABLE RECTANGULAR CAVITY

MODE / CONFIGURATION	100	010	110	210
12" x 5.5 " x 2.5"	564 Hz	1232 Hz	1355 Hz	1671 Hz
12" x 5.75" x 2.5"	564	1178	1306	1632
12" x 6.0 " x 2.5"	564	1129	1262	1597
12" x 6.25" x 2.5"	564	1083	1222	1565
12" x 6.5 " x 2.5"	564	1042	1185	1536
12" x 6.75" x 2.5"	564	1004	1151	1510
12" x 7.0 " x 2.5"	564	968	1120	1487

TABLE I. THEORETICALLY PREDICTED MODES

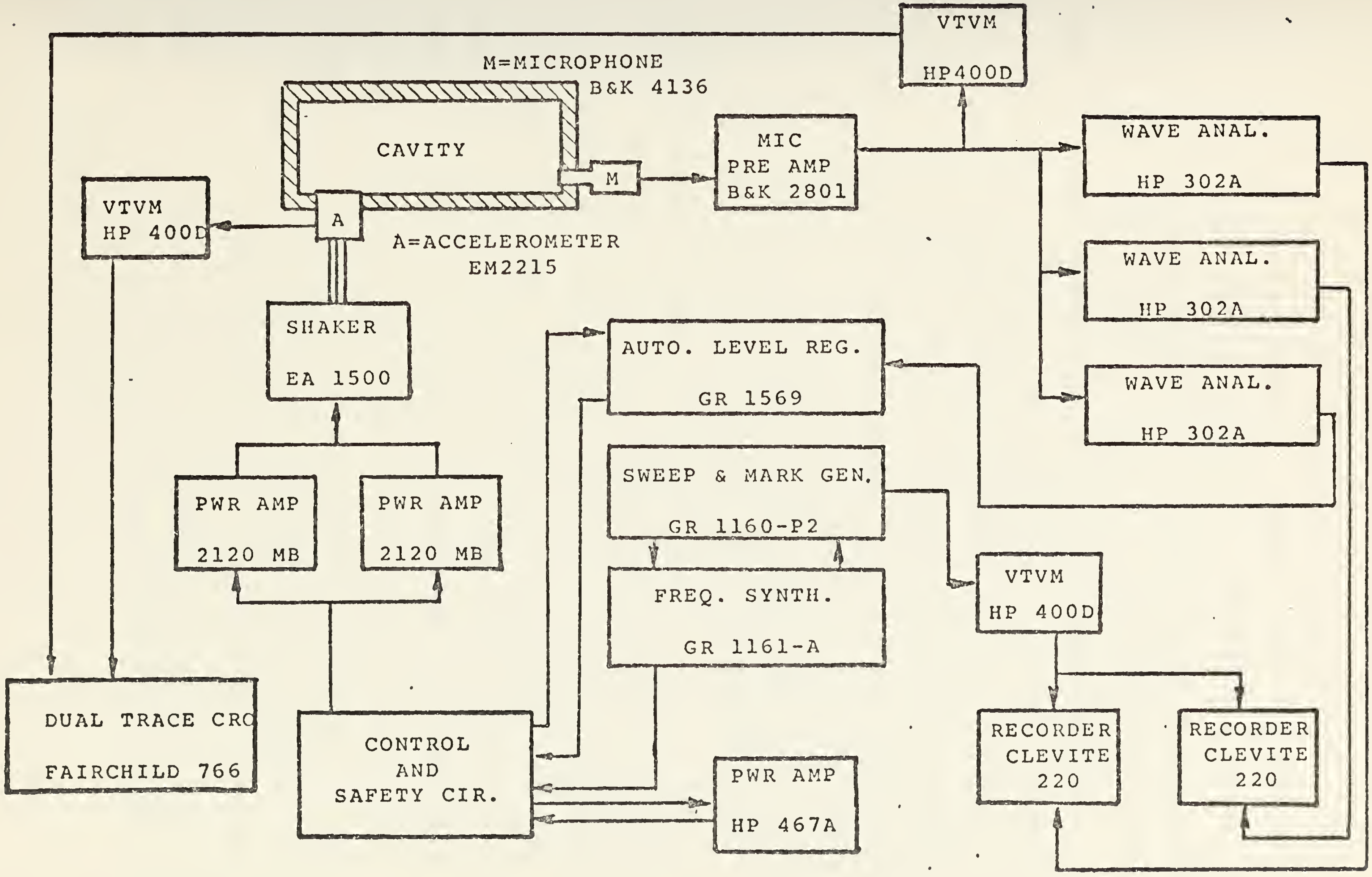

FIGURE 2. APPARATUS BLOCK DIAGRAM

Exciter which, in turn was driven by two M-B Electronics Model 2120MB Power Amplifiers operating in parallel. The driving signal was produced by a General Radio 1161-A Coherent Decade Frequency Synthesizer, configured to provide frequencies precise to 0.001 Hz. A General Radio Model 1160P2 Sweep and Marker Generator and Model GR1569 Automatic Level Regulator made automatic collection of data possible.

The piston movement was continuously monitored by means of an Endevco Model 2215 Accelerometer mounted within the piston. The output voltage of this accelerometer was measured on a Hewlett Packard Vacuum Tube Voltmeter Model HP400D, and the output of this meter displayed on a Fairchild Model 776H Dual-trace Oscilloscope. (The input impedance of the oscilloscope was too low to allow the accelerometer to be directly connected to the oscilloscope.)

The sound pressure in the cavity was sensed by the Bruel and Kjaer type 4136 condenser microphone with matching preamplifier type 2801. The output of this preamplifier went to five other pieces of equipment. (1) A Hewlett Packard HP400D VTVM to measure the overall voltage level. (2) Second input of the Fairchild Oscilloscope. This allowed a continuous display of the acoustic signal present in the cavity. The oscilloscope was externally triggered by the output of the synthesizer. (3-5) Three Hewlett Packard HP302A Wave Analyzers with 7Hz bandwidth set to AFC (Automatic Frequency Control), so that they automatically followed the selected signal as the frequency slowly varied.

Two of the wave analyzers were set to the second and third harmonic of the sound signal. Their outputs were passed to two Clevite Brush Recorders Model 220, and a time record of the second and third harmonic signal contents were printed on one channel of the paper tape of their respective recorders.

The output of the third wave analyzer, set to the fundamental frequency, was used as a control signal for the Automatic Level Regulator. The Regulator controlled the driving level to the 2120MB Power Amplifiers, so that the level of the first harmonic remained constant while the frequency was swept through a cavity resonance. The Sweep and Marker Generator was used to automatically sweep the frequency about a set center frequency. The Sweep Generator has various sweep speeds and produces a marker signal at the center frequency,as well as at set intervals. The marker signal, amplified by a HP400D VTVM, was passed to the second channels of both Brush Recorders. (It was necessary to amplify the marker signal because the Sweep Generator was operated at its lowest speed, where the marker voltage was insufficient to produce a mark.)

The final element in the experimental setup was a control and safety circuit specifically designed and constructed for this project. This circuit performed three basic tasks. The first was a switching function that allowed connection of all the appropriate signals to the equipment so the

Automatic Level Regulator maintained control of the drive level. The opposite switch position bypassed the Regulator completely and allowed the drive signal to be controlled at the Frequency Synthesizer.

The second function of this circuit was to provide a safety relay. Since the output of the Level Regulator is inversely proportional to the voltage of the control signal, loss of that signal causes the Regulator to output its maximum voltage to the 2120MB Power Amplifiers. To prevent possible damage, the safety circuit monitors the signal to the power amplifiers and removes this signal wherever it exceeds a value set by the Associated Hewlett Packard HP467A Power Amplifier as shown in Figure 2. Once the circuit is tripped, indicated by a panel light, it remains open until reset by the safety circuit/bypass switch.

The last job performed by the control and safety circuit is that of a variable attenuator, which allows the operating voltage levels of the Regulator to be maintained near its mid-scale range. This also provides an inherent safety feature by limiting the maximum drive signal. This feature could also be bypassed.

B. STRENGTH PARAMETER AND MICROPHONE SENSITIVITY

The strength parameter defined as

$$SP = MbQ_1 ,$$

where

$$M = P_1/\rho c^2$$

is the basic quantity which characterizes the strength of the finite-amplitude interaction. To determine SP, it is necessary to know P_1, which in turn can be calculated from the microphone output voltage if the microphone sensitivity is known. Microphone sensitivity, obtained with a Breul and Kjaer Model 4220 pistonphone, was found to be

$$S_M = (1.56 \pm 0.03) \times 10^{-3}\ \mathrm{VOLT}/(\mathrm{nT}/\mathrm{M}^2).$$

Using the relationships

$$S_M = V_M/P_{rms}$$

and

$$P_1 = \sqrt{2}\ P_{rms}$$

one can rewrite the strength parameter as

$$SP = (7.62 \times 10^{-3})\ V_M Q_1\ ,$$

where V_M is the rms voltage of the fundamental.

C. FREQUENCY PARAMETER

The frequency parameter, defined by

$$FP = 2(f_n - nf_1)\ Q_1/nf_1\ ,$$

normalizes the driving frequency to the fundamental resonance of the system. For example, FP equal to ± 1.00 corresponds to driving the cavity at the 1/2-power point of the fundamental resonance.

D. AUTOMATIC DATA COLLECTION

Previous investigations [3,4,12,14] encountered a drift of the resonant frequencies. Slight temperature changes were postulated to be the cause. To minimize this effect the system was allowed to warm up by driving the cavity for four hours at a strength parameter approximately equal to those to be investigated. This significantly reduced the rate of frequency drift. This, coupled with the 10- to 20-fold decrease in run time that automatic data collection provided, greatly reduced frequency drift from 0.8Hz per run to less than 0.05Hz per run.

Another advantage of this automated system was the simultaneous recording of harmonics as a continuous function of frequency. The number of harmonics investigated during any one run was limited only to the number of available HP302A Wave Analyzers and Brush Recorder channels.

E. SYSTEM ALIGNMENT

The primary factor in setting the lower limit to the measurement of harmonic content was the amount of distortion injected into the cavity by the piston. Misalignment of the piston within its port causes distortion of the piston motion which was detected by analyzing the harmonic content of the accelerometer output voltage. (With the piston removed from its port, distortion levels were of the same order of magnitude as the general electronic noise level of the accelerometer system when at rest.) Before each run, the piston was

aligned within its port so that the accelerometer output voltage contained less than 0.1% second harmonic and 0.2% third harmonic.

After testing various configurations, the one selected for ease of alignment consisted of the cavity mounted on a tripod support directly above the exciter, which was supported by its own base in an upright position. Both the cavity tripod and the exciter rested on a 5/16 in. pad of stiff acoustic rubber. Once the system was aligned, only an occasional minor adjustment was necessary to maintain low piston distortion.

IV. DATA COLLECTION PROCEDURES

A. PRERUN PROCEDURES

Because the system was designed to collect the bulk of the data automatically, careful attention to prerun procedures was essential for an accurate data run. The system was warmed up for at least four hours prior to any final run preparations, so as to keep any frequency drift to a minimum. After this warm up period and prior to anything else, the piston motion was analyzed using the HP302A Wave Analyzers, and the system aligned as necessary.

The HP302A's were then reconnected to monitor the microphone output and set to track (AFC position of function switch) the fundamental, second, and third harmonic frequencies. Next, the Frequency Synthesizer was set to the resonance frequency of the gravest member of the family to be investigated, and the signal amplitude was adjusted until the value of the fundamental voltage reached the desired level. The ratios of each harmonic to the fundamental was calculated from the wave analyzer, and an appropriate scale was selected for each Brush Recorder so that the stylus was approximately at its maximum position. Once the Brush Recorders were set they did not need to be recalibrated as long as the fundamental voltage was maintained at the prescribed level.

The Sweep and Marker Generator was set to sweep a frequency band equivalent to ± 3.0 in frequency parameter centered at the resonant frequency, and an appropriate marker spacing was set. The sweep was momentarilly stopped while the Automatic Level Regulator was switched into the circuit and brought up to the prescribed voltage level. (Maximum stable regulation rate was 10 dB/sec.) The automatic sweep was then allowed to continue, and the output of the 2120MB Power Amplifiers was carefully monitored to prevent accidental overdriving of the EA1500 Excitor. Sweep speed of sixty seconds, and tape speed of 5mm/sec were used and the system was allowed to make two full sweeps, at which time Recorder calibration and stability of the fundamental voltage level was checked. If all systems were properly operating, the time was recorded and the system made its final two frequency sweeps while the fundamental voltage level was continuously monitored for any undesired change.

B. RUN SEQUENCE

The run officially began when the final two frequency sweeps commenced. (All previous recordings were discarded to prevent confusion due to possible frequency drift.) Upon completion of the final two frequency sweeps, the second phase of the measurements followed immediately. The Automatic Level Regulator and Sweep Generator were switched out of the system, and the Frequency Synthesizer was used alone to carry out the infinitesimal amplitude analysis. Detailed

measurements of the Q and E for the fundamental, each recorded mode, and, where possible, modes of higher order were performed. In measuring the Q_1, it was necessary to maximize the microphone output voltage by varying the frequency. Then the frequency was shifted off resonance until the voltage was -3dB below the maximum. The difference between the -3dB points on both sides of the maximum determined the bandwidth (Δf), and, assuming the resonance frequency was exactly between these two, allowed the calculation of Q. In those cases where degenerate modes appeared and -3dB down frequencies could not be achieved, the -1dB and -2dB points were measured for both the family and degenerate modes and their center frequencies and Q's could be extrapolated using a method described by Devall [5]. Since Q measurements were observed to be very similar between the runs for both cavity configurations, the average values for Q of the non-degenerate modes were used as the computer input parameters for those modes where degeneracies impaired the measurements. An average set of Q and E measurements took from five to six minutes. With the present automatic collection system, increasing the number of harmonics recorded by the addition of more analyzers and recording channels will not effect the actual run time.

V. RESULTS

Tables II through V display the properties of the cavity determined from infinitismal-amplitude measurements for each run. The tables represent one- and two-dimensional modes (n00 and nn0) for the non-degenerate and degenerate configurations (A and B respectively). Each table lists the strength parameter (SP) of the various runs, and contains the center frequency of the n^{th} harmonic (f_{0n}) along with their measured bandwidths (Δf), Q's, and E's.

The theoretical values for harmonic content were calculated using the values found in these tables. Cavity configuration B's design specifications required the 200 and 010, 400 and 020, 500 and 320, and 220 and 410 modes to be degenerate pairs. Data were taken, and theoretical curves generated in both configurations for strength parameters of about 0.29, 0.38, 0.47 (B only), 0.55, and 0.65 driving the 100 mode and 0.24, 0.37, and 0.49 for driving the 110 mode. In all runs the piston was positioned with its face flush with the interior floor of the cavity.

Figures 3 through 17 display the experimentally measured harmonic distortion (dashed line) and the theoretically predicted values (dotted line). With few exceptions, theoretical and experimental values lie well within experimental error limits. For Figures 7, 8, 9, 10, 11, 15, 16 and 17,

TABLE II

n00 Modes CONFIGURATION A (12"x5.75"x2.5")

SP	RUN#	n	f_{0n} (Hz)	Δf (Hz)	Q(n)	E(n) ($\times 10^{-3}$)
0.295	5	1	568.01	2.20	257	0.0
		2	1136.64	3.08	388	0.536
		3	1705.14	3.87	439	0.648
		4	2273.89	4.38	516	0.809
(fig.3)						
0.380	1	1	565.64	2.26	249	0.0
		2	1131.90	3.08	367	0.551
		3	1697.77	3.80	447	0.507
		4	2264.17	4.53	511	0.644
(fig.4)						
0.551	3	1	568.17	2.36	241	0.0
		2	1137.12	3.12	364	0.688
		3	1705.76	3.91	436	0.736
		4	2274.86	4.40	517	0.966
(fig.5)						
0.651	4	1	568.14	2.34	244	0.0
		2	1137.03	3.09	367	0.637
		3	1705.58	3.87	440	0.362
		4	2274.62	4.42	514	0.912
(fig.6)						

TABLE III

n00 MODES CONFIGURATION B (12"x6.0"x2.5")

SP	RUN#	n	f_{0n} (Hz)	Δf (Hz)	Q(n)	E(n) ($\times 10^3$)
0.292	9	1	566.81	2.22	255	0.0
		2	1134.84	3.40	334	1.08
		3	1701.66	3.77	451	0.725
		4	2270.07	4.43	512	1.25
(fig.7)						
0.381	11	1	566.82	2.27	249	0.0
		2	1134.90	3.48	326	1.10
		3	1701.78	3.86	440	0.771
		4	2270.26	4.45	510	1.31
(fig.8)						
0.473	12	1	566.94	2.28	248	0.0
		2	1135.17	3.47	326	1.14
		3	1702.19	3.86	441	0.808
		4	2270.83	4.46	509	1.36
(fig.9)						
0.559	13	1	564.50	2.31	244	0.0
		2	1130.34	3.35	337	1.19
		3	1695.06	3.80	446	0.927
		4	2261.44	4.39	513	1.53
(fig.10)						
0.651	14	1	564.93	2.32	244	0.0
		2	1131.23	3.45	328	1.22
		3	1696.30	3.86	439	0.887
		4	2263.05	4.45	508	1.47
(fig.11)						

TABLE IV

nn0 MODES CONFIGURATION A (12"x5.75"x2.5")

SP	RUN#	n	f_{0n} (Hz)	Δf (Hz)	Q(n)	E(n) (x10^3)
0.255	8	1	1309.28	3.91	335	0.0
		2	2629.16	5.26	486	0.608
		3	3930.70	7.43	519	0.725
(fig.12)						
0.382	6	1	1310.18	3.92	334	0.0
		2	2621.67	5.58	481	0.499
		3	3932.90	7.63	516	0.599
(fig.11)						
0.504	7	1	1308.12	3.96	330	0.0
		2	2617.87	5.29	494	0.620
		3	3927.48	7.45	527	0.793
(fig.12)						

TABLE V

nn0 MODES CONFIGURATION B (12"x6.0"x2.5")

SP	RUN#	n	f_{0n} (Hz)	Δf (Hz)	Q(n)	E(n) ($\times 10^3$)
0.240	15	1	1263.38	4.01	315	0.0
		2	2527.79	5.20*	486*	0.406
		3	3793.84	7.04	538	0.975
(fig.15)						
0.360	16	1	1265.96	4.01	315	0.0
		2	2532.95	5.21*	486*	0.404
		3	3801.56	7.05	539	0.967
(fig.16)						
0.476	18	1	1267.64	4.11	307	0.0
		2	2536.31	5.22*	486*	0.403
		3	3803.72	6.78	552	0.207
(fig.17)						

*These values were obtained from averaging the Q's for the same mode from configuration A.

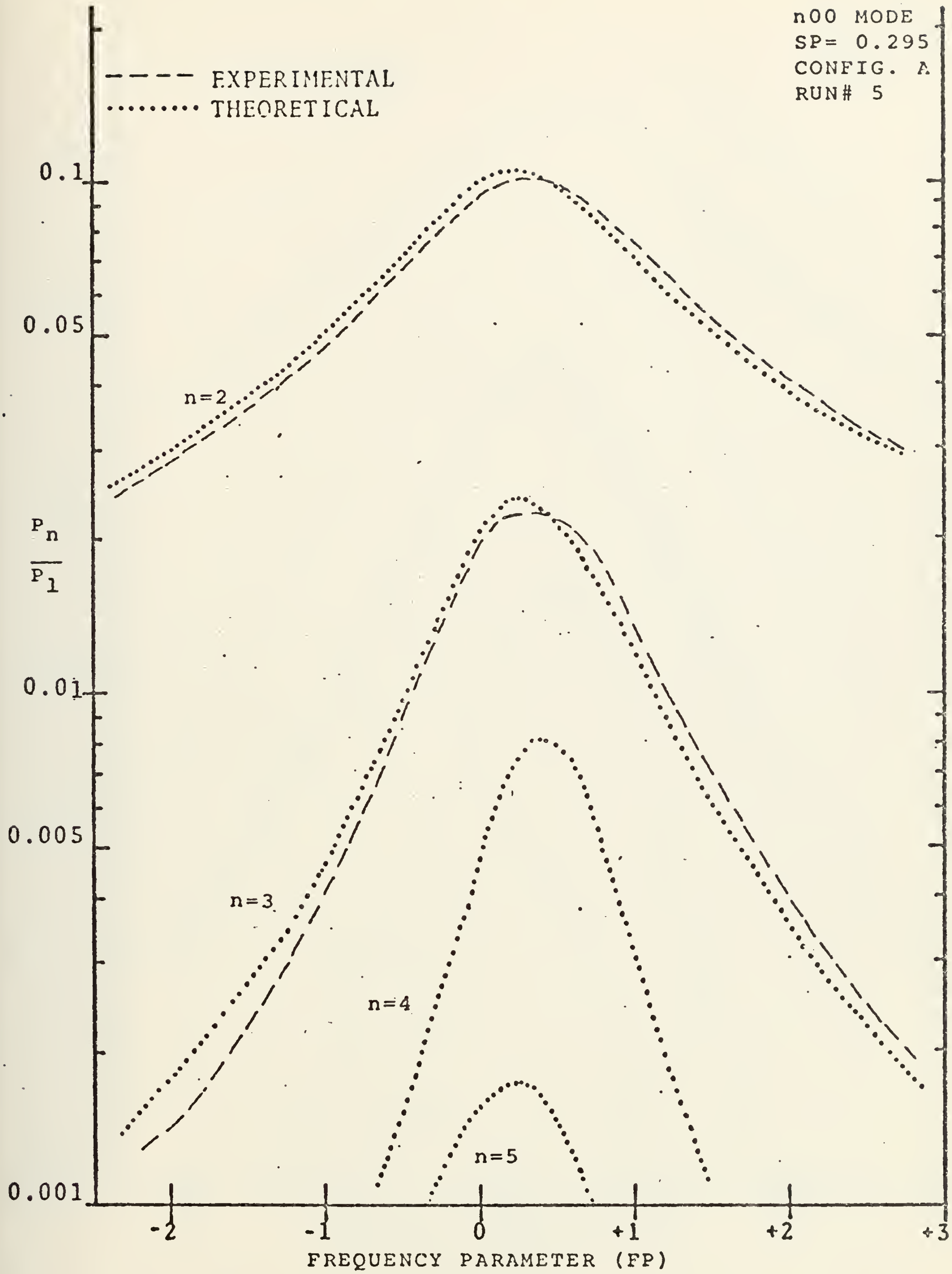

n00 MODE
SP= 0.295
CONFIG. A
RUN# 5
EXPERIMENTAL
THEORETICAL
0.1
0.05
0.01
0.005
0.001
$\frac{P_n}{P_1}$
n=2
n=3
n=4
n=5
-2
-1
0
+1
+2
+3
FREQUENCY PARAMETER (FP)

FIGURE 3

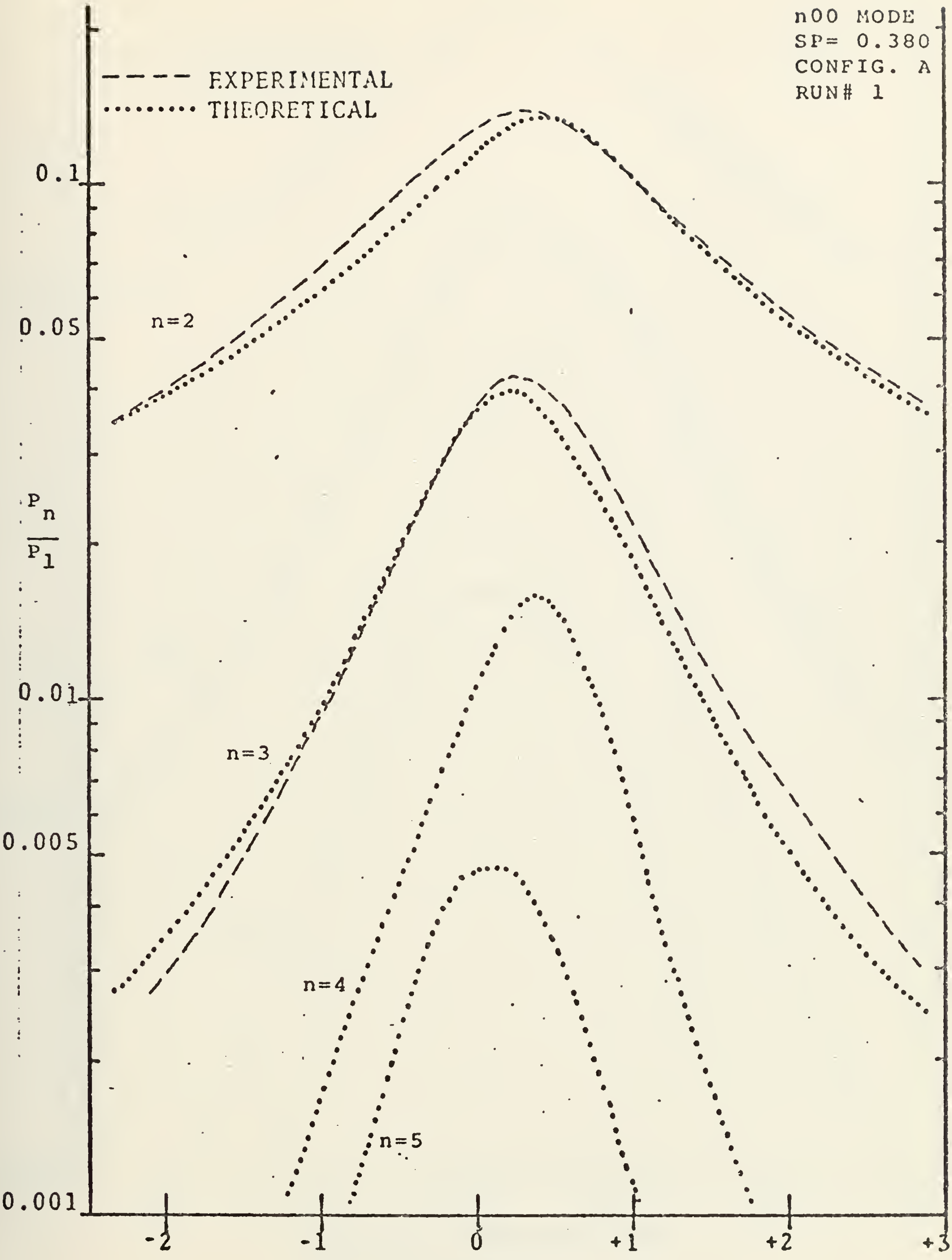

---- EXPERIMENTAL
.... THEORETICAL
n00 MODE
SP= 0.380
CONFIG. A
RUN# 1
$\frac{P_n}{P_1}$
0.1
0.05
0.01
0.005
0.001
n=2
n=3
n=4
n=5
-2
-1
0
+1
+2
+3
FREQUENCY PARAMETER (FP)

FIGURE 4

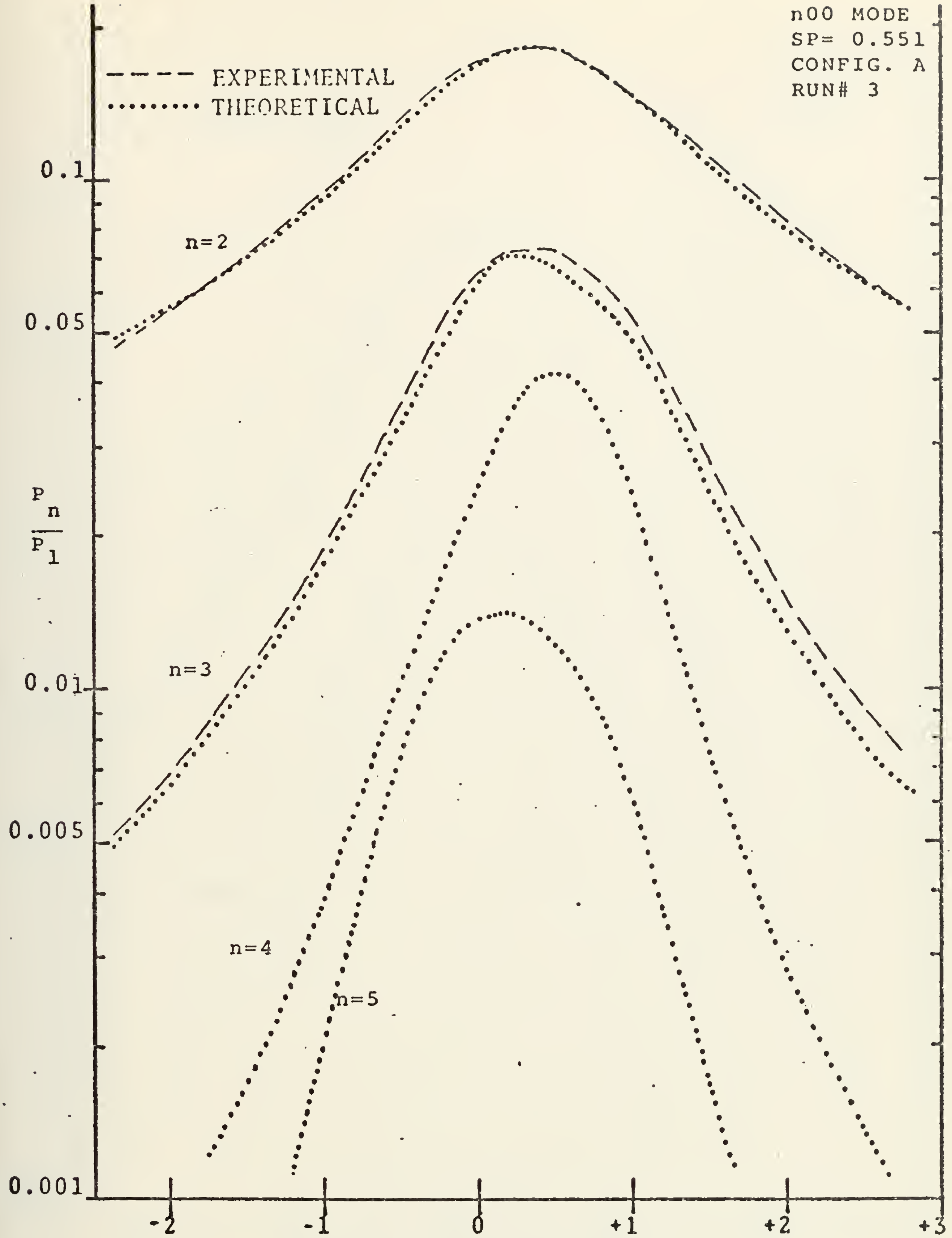n00 MODE
SP= 0.551
CONFIG. A
RUN# 3
EXPERIMENTAL
THEORETICAL
0.1
0.05
0.01
0.005
0.001
$\frac{P_n}{P_1}$
n=2
n=3
n=4
n=5
-2
-1
0
+1
+2
+3
FREQUENCY PARAMETER (FP)

FIGURE 5

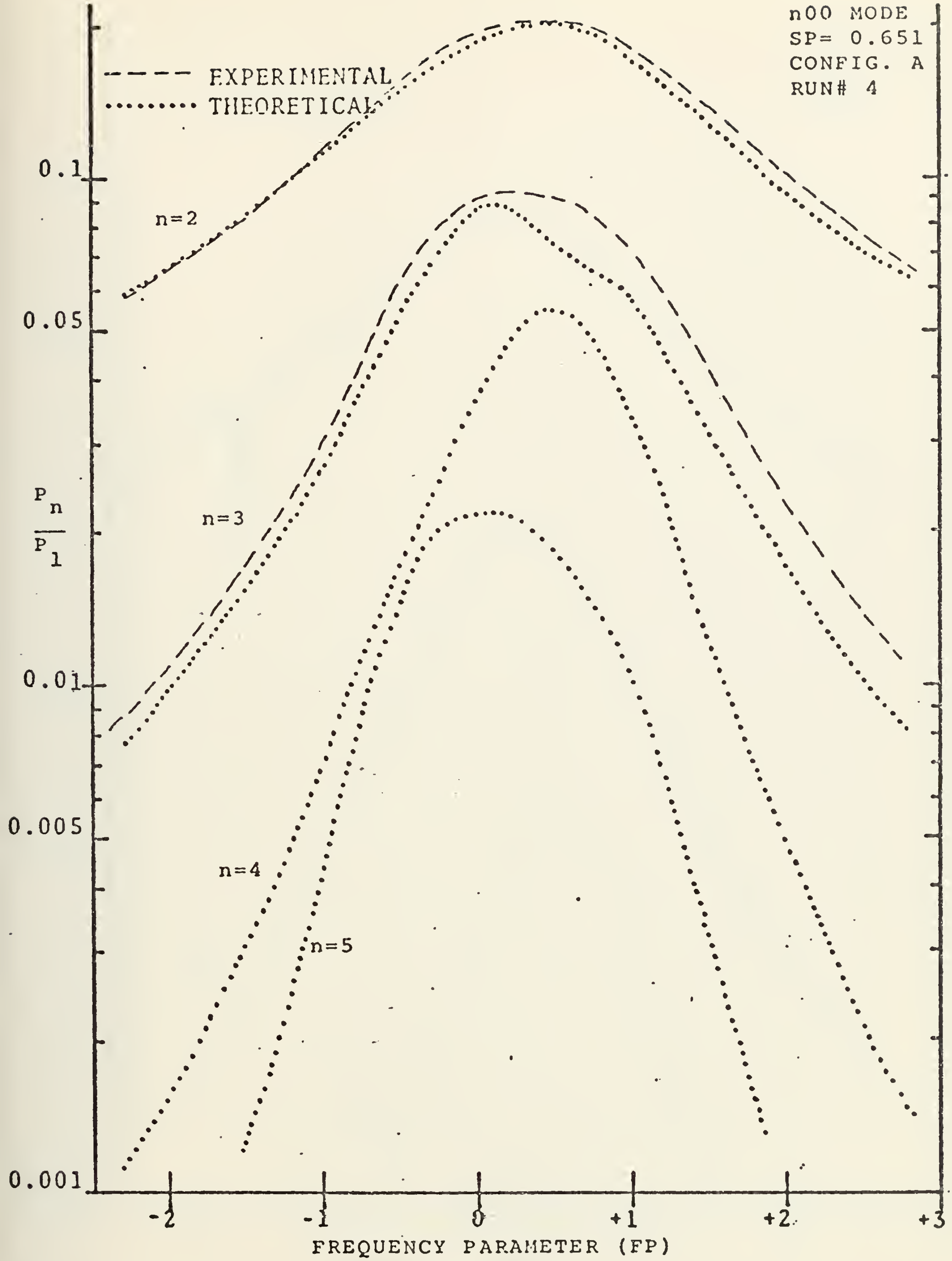
n00 MODE
SP= 0.651
CONFIG. A
RUN# 4
EXPERIMENTAL
THEORETICAL
n=2
n=3
n=4
n=5
$\frac{P_n}{P_1}$
0.1
0.05
0.01
0.005
0.001
-2
-1
0
+1
+2
+3
FREQUENCY PARAMETER (FP)

FIGURE 6

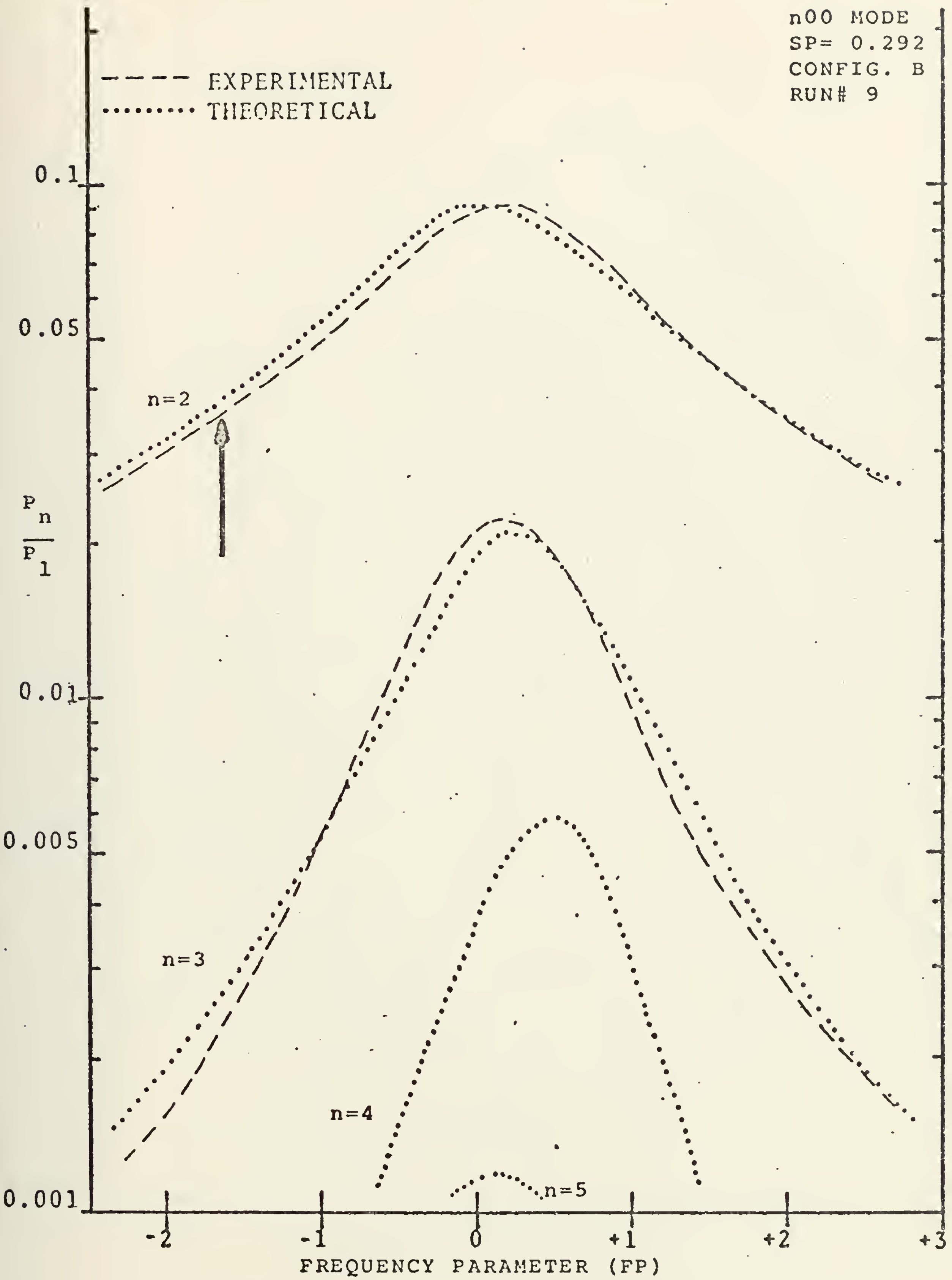
n00 MODE
SP= 0.292
CONFIG. B
RUN# 9
- - - - EXPERIMENTAL
.... THEORETICAL
0.1
0.05
0.01
0.005
0.001
$\frac{P_n}{P_1}$
n=2
n=3
n=4
n=5
-2
-1
0
+1
+2
+3
FREQUENCY PARAMETER (FP)

FIGURE 7

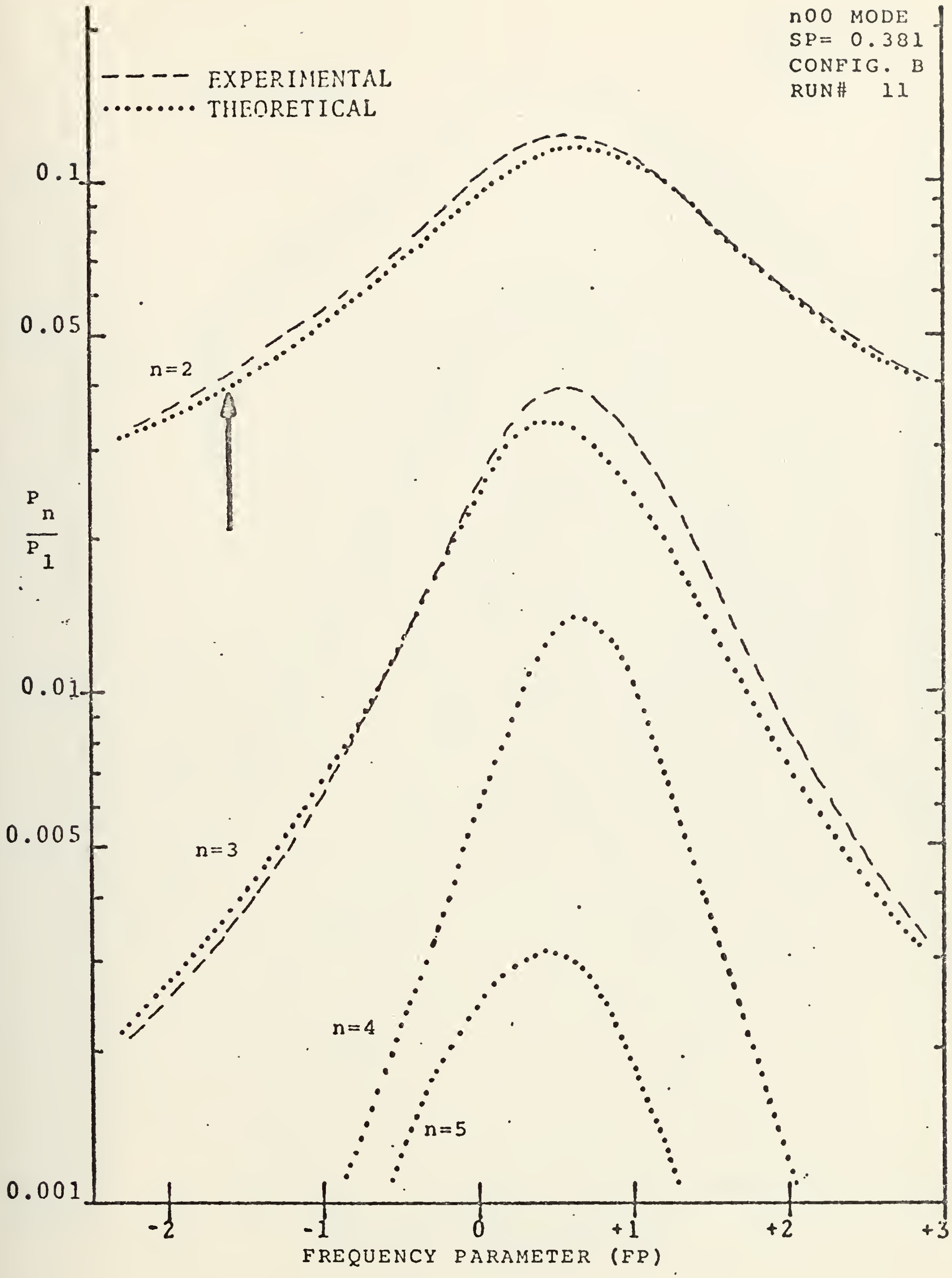
n00 MODE
SP= 0.381
CONFIG. B
RUN# 11
EXPERIMENTAL
THEORETICAL
0.1
0.05
0.01
0.005
0.001
$\frac{P_n}{P_1}$
n=2
n=3
n=4
n=5
-2
-1
0
+1
+2
+3
FREQUENCY PARAMETER (FP)

FIGURE 8

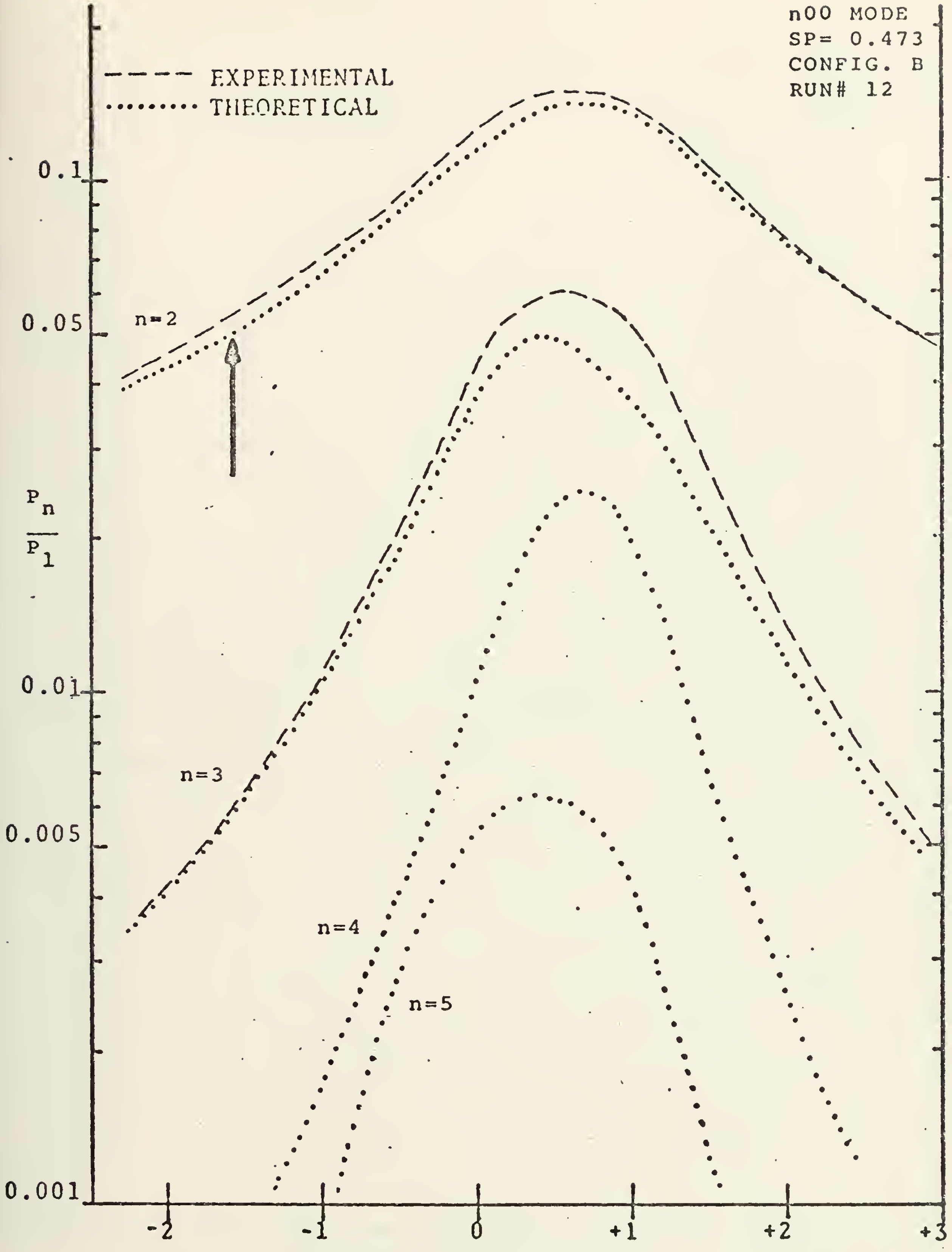

n00 MODE
SP= 0.473
CONFIG. B
RUN# 12
EXPERIMENTAL
THEORETICAL
0.1
0.05
0.01
0.005
0.001
$\frac{P_n}{P_1}$
n=2
n=3
n=4
n=5
-2
-1
0
+1
+2
+3
FREQUENCY PARAMETER (FP)

FIGURE 9

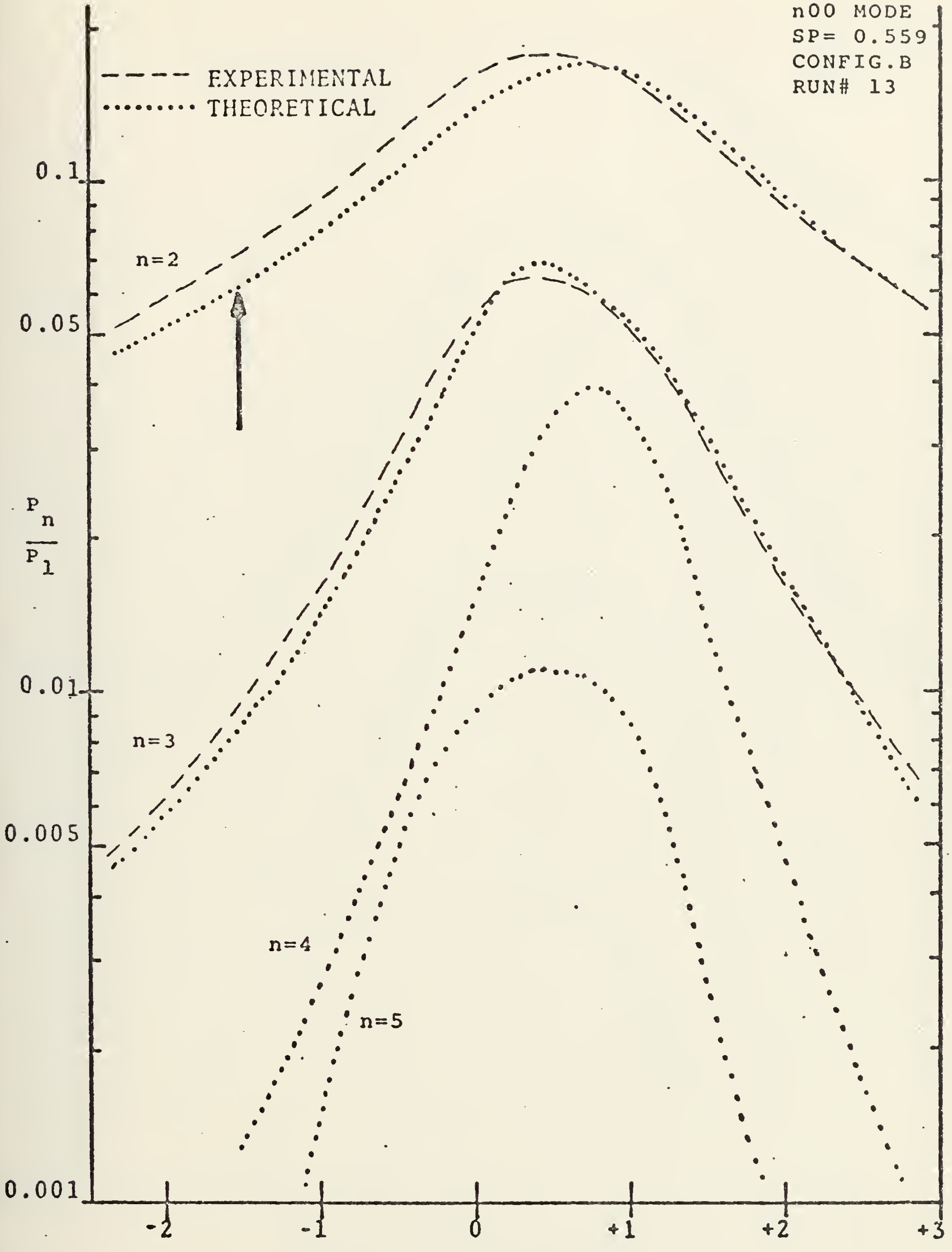

n00 MODE
SP= 0.559
CONFIG.B
RUN# 13
EXPERIMENTAL
THEORETICAL
0.1
0.05
0.01
0.005
0.001
$\frac{P_n}{P_1}$
n=2
n=3
n=4
n=5
-2
-1
0
+1
+2
+3
FREQUENCY PARAMETER (FP)

FIGURE 10

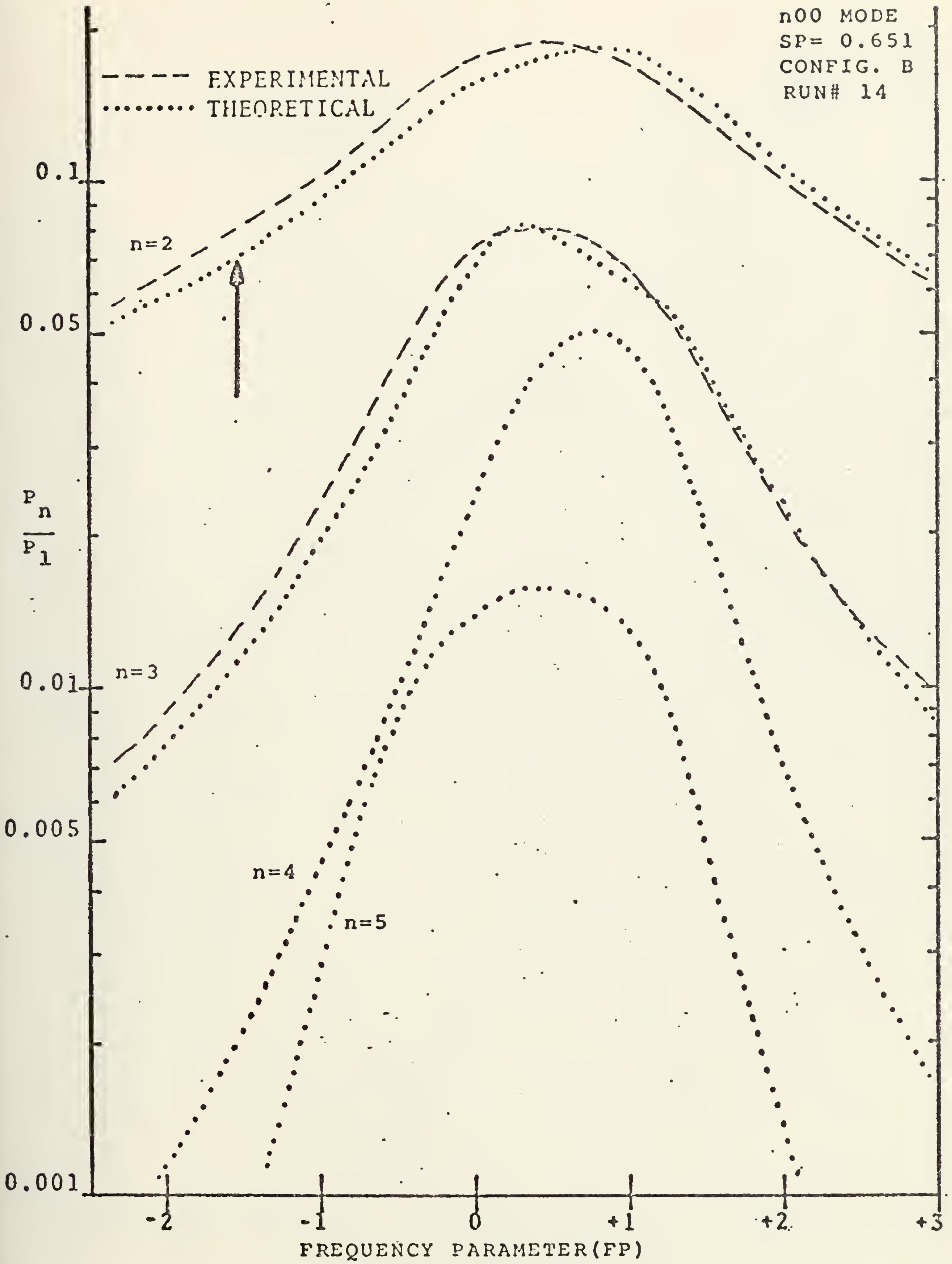
n00 MODE
SP= 0.651
CONFIG. B
RUN# 14
EXPERIMENTAL
THEORETICAL
n=2
n=3
n=4
n=5
0.1
0.05
0.01
0.005
0.001
$\frac{P_n}{P_1}$
-2
-1
0
+1
+2
+3
FREQUENCY PARAMETER(FP)

FIGURE 11

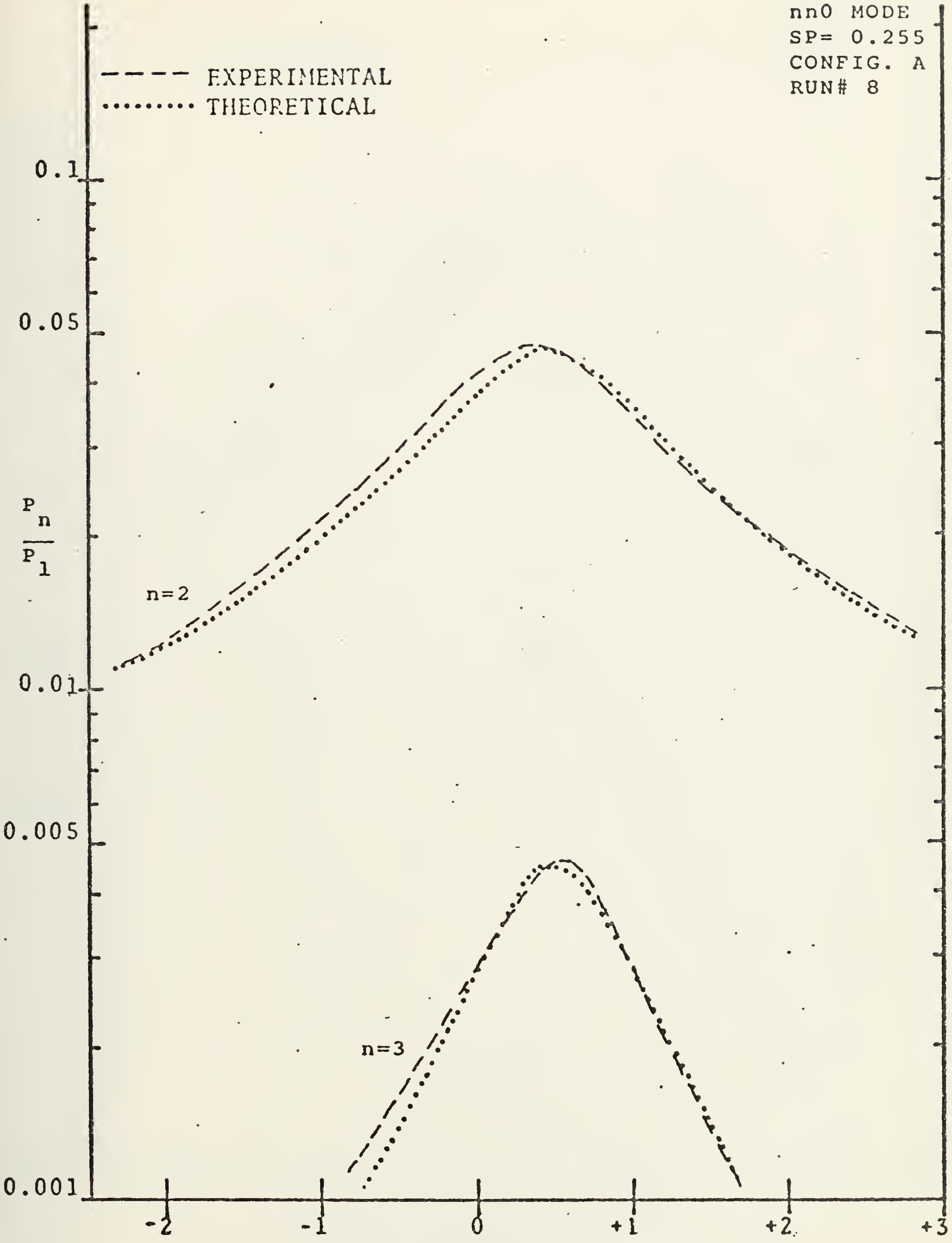

nn0 MODE
SP= 0.255
CONFIG. A
RUN# 8
---- EXPERIMENTAL
········ THEORETICAL
0.1
0.05
0.01
0.005
0.001
$\frac{P_n}{P_1}$
n=2
n=3
-2
-1
0
+1
+2
+3
FREQUENCY PARAMETER (FP)

FIGURE 12

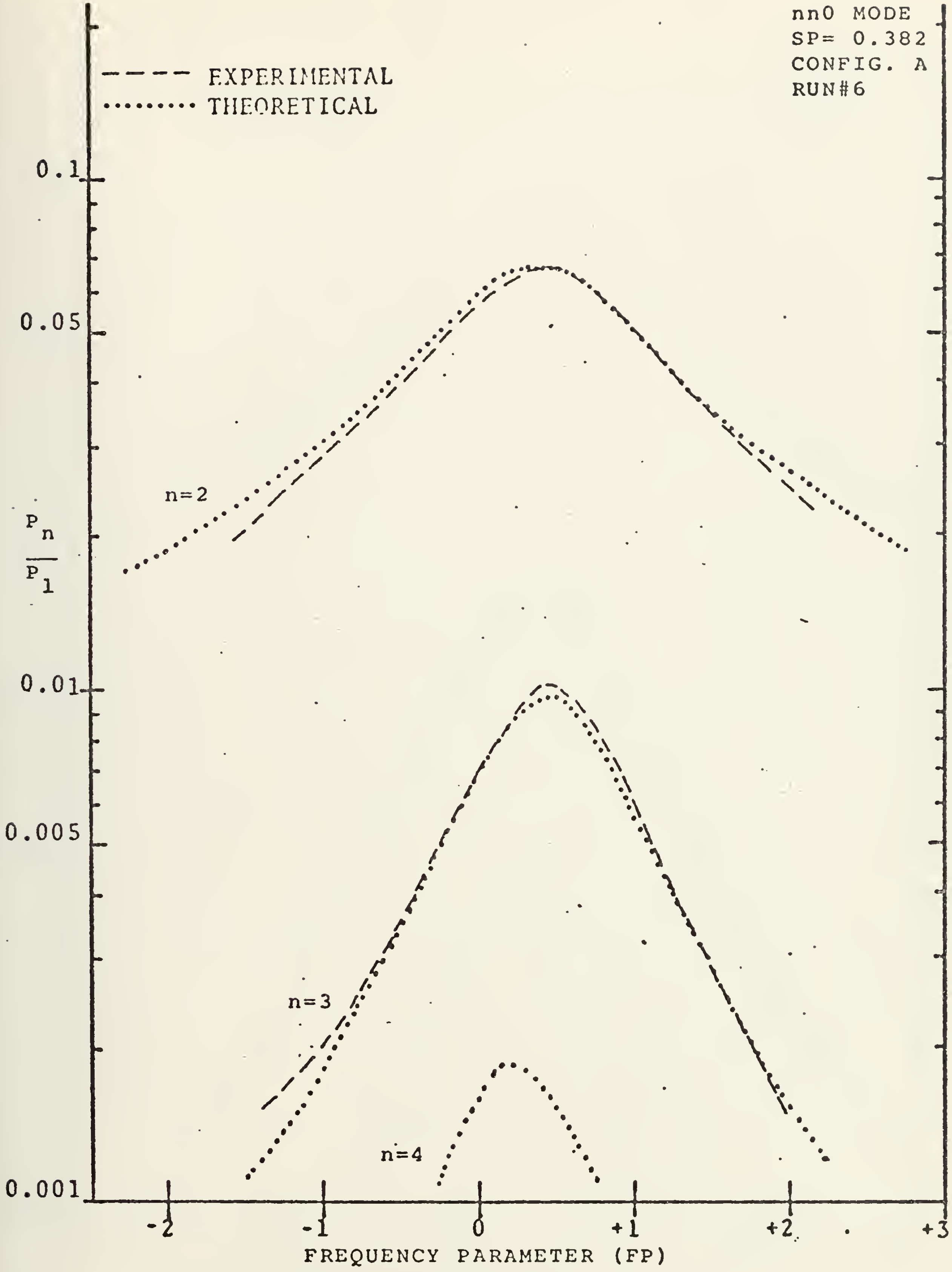nn0 MODE
SP= 0.382
CONFIG. A
RUN#6
EXPERIMENTAL
THEORETICAL
0.1
0.05
0.01
0.005
0.001
$\frac{P_n}{P_1}$
n=2
n=3
n=4
-2
-1
0
+1
+2
+3
FREQUENCY PARAMETER (FP)

FIGURE 13

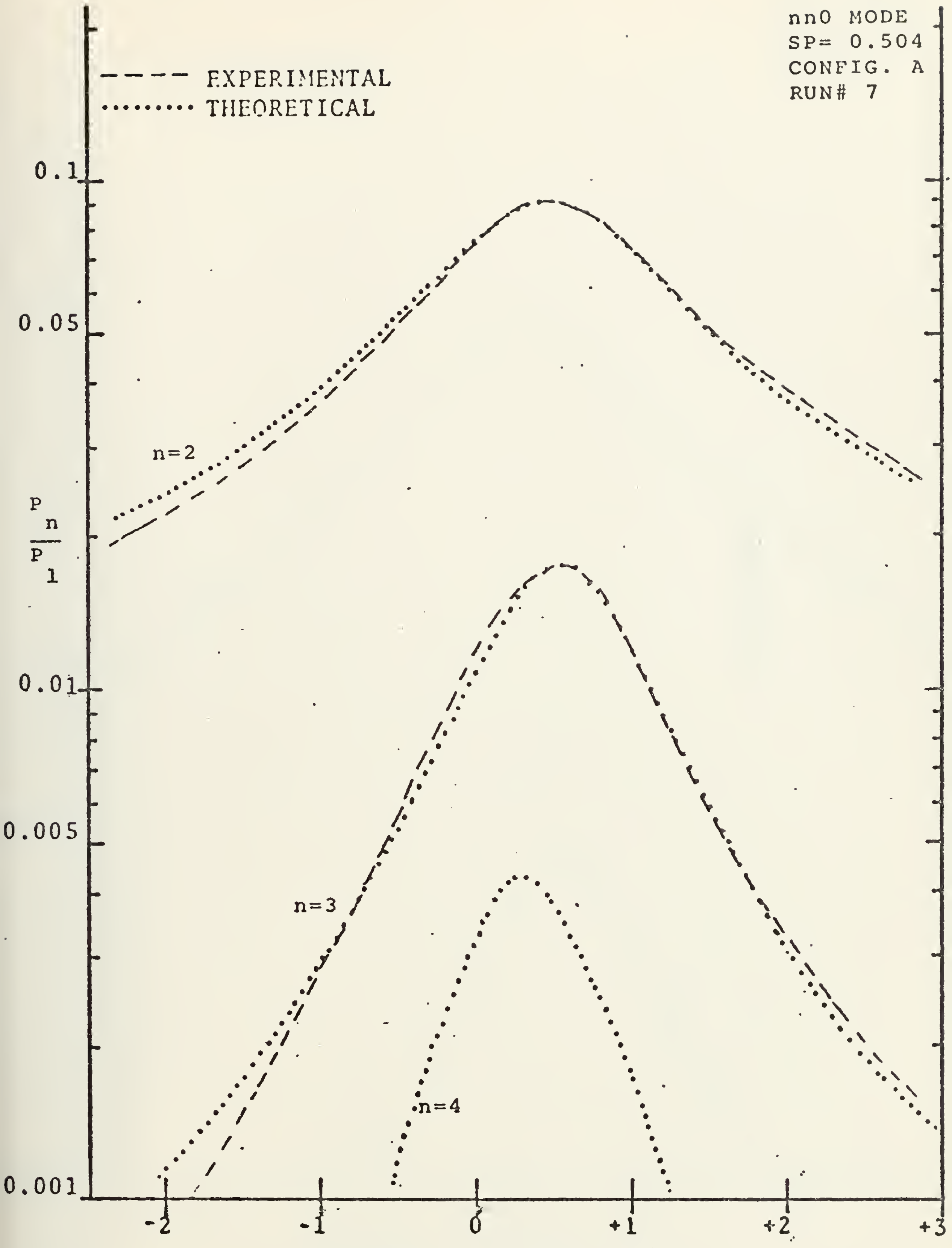

---- EXPERIMENTAL
········ THEORETICAL
nn0 MODE
SP= 0.504
CONFIG. A
RUN# 7
0.1
0.05
0.01
0.005
0.001
P_n/P_1
n=2
n=3
n=4
-2
-1
0
+1
+2
+3
FREQUENCY PARAMETER (FP)

FIGURE 14

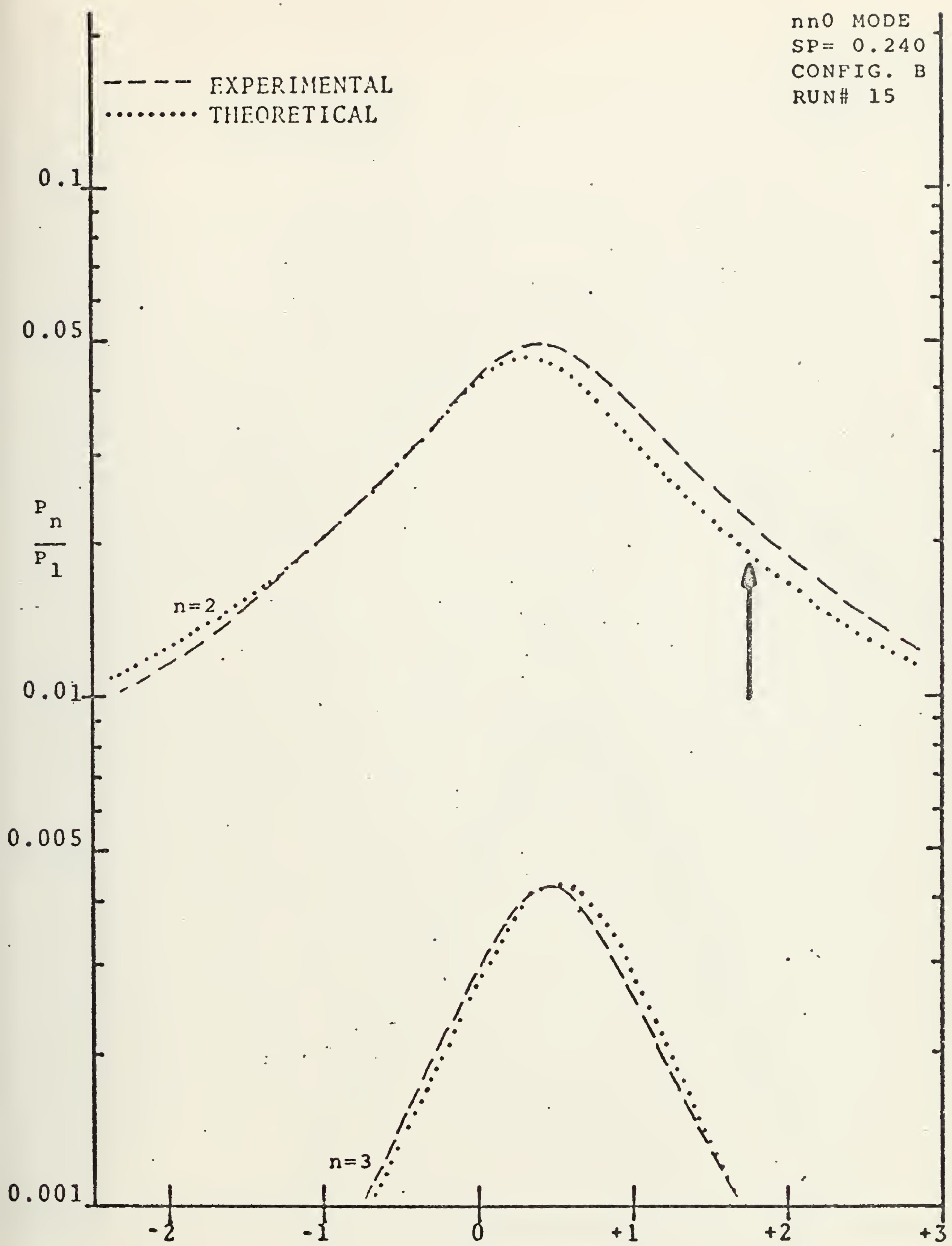
---- EXPERIMENTAL
········ THEORETICAL
nn0 MODE
SP= 0.240
CONFIG. B
RUN# 15
0.1
0.05
0.01
0.005
0.001
$\frac{P_n}{P_1}$
n=2
n=3
-2
-1
0
+1
+2
+3
FREQUENCY PARAMETER (FP)

FIGURE 15

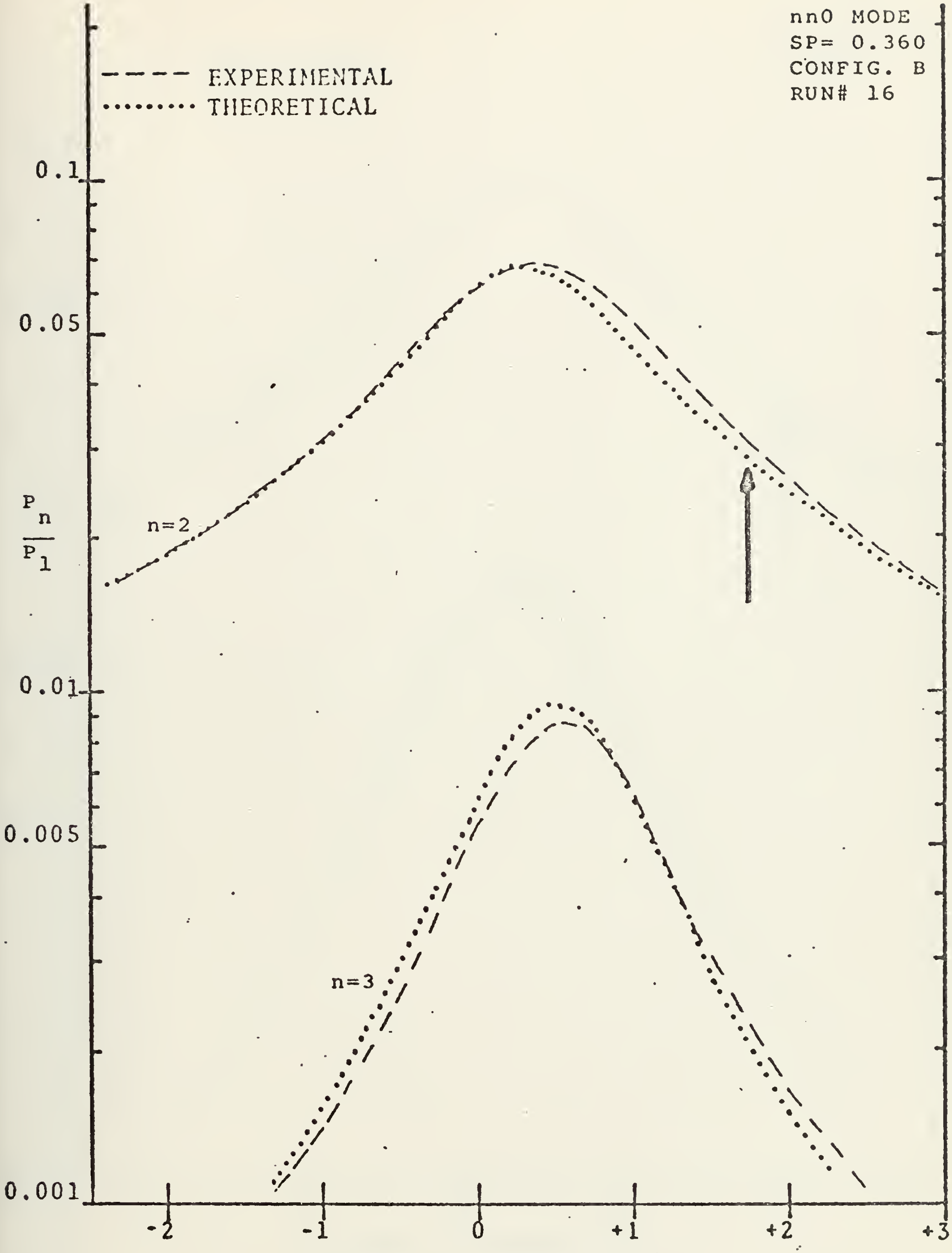

---- EXPERIMENTAL
········ THEORETICAL
nn0 MODE
SP= 0.360
CONFIG. B
RUN# 16
0.1
0.05
0.01
0.005
0.001
$\frac{P_n}{P_1}$
n=2
n=3
-2
-1
0
+1
+2
+3
FREQUENCY PARAMETER (FP)

FIGURE 16

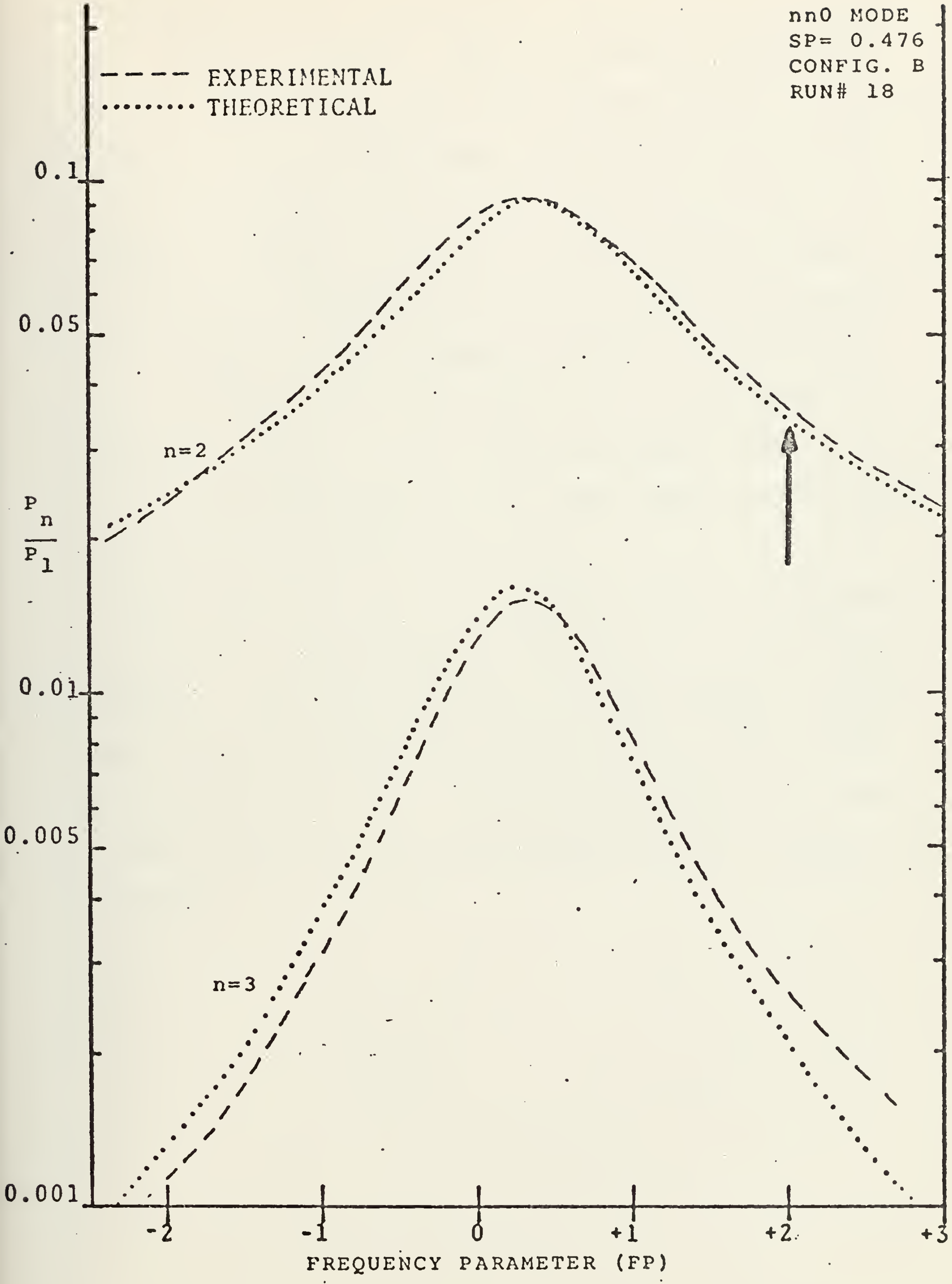
nn0 MODE
SP= 0.476
CONFIG. B
RUN# 18
---- EXPERIMENTAL
········ THEORETICAL
0.1
0.05
0.01
0.005
0.001
$\frac{P_n}{P_1}$
n=2
n=3
-2
-1
0
+1
+2
+3
FREQUENCY PARAMETER (FP)

FIGURE 17

arrows indicate the locations of the associated degeneracies. Tables VI and VII list the resonance frequencies and Q's of the driving mode, the center frequencies and the value of FP at which the mode would peak for each degenerate pair. (A perfectly tuned cavity with no wall losses would exhibit a frequency parameter of zero for these frequencies.) One point of considerable interest is that on all figures for the degenerate configuration (Figures 7-11, 15-17), there is no observable deviation of the experimental and theoretical curves for the second harmonic. This is true for the one-dimensionally driven mode (100) as well as the two-dimensionally driven one (110).

The only significant discrepancies appear in Figures 5, 6, 9, and 10, near the peaks of the curves for the third harmonics. The theory predicts a significantly flat response for these higher strength parameters that was not observed experimentally. It is also interesting to note the peak position of the fifth harmonic and its effect on the fourth.

TABLE VI

DEGENERATE PAIRS, 100 DRIVEN MODE

RUN#	$f_{(100)}$	Q_1	$f_{(200)}$	FP	$f_{(010)}$	FP
9	566.81 Hz	255	1134.84 Hz	+0.53	1130.02 Hz	-1.62
11	566.82	249	1134.90	+0.55	1130.08	-1.57
12	566.94	248	1135.17	+0.56	1130.36	-1.44
13	564.50	244	1130.34	+0.58	1125.53	-1.50
14	564.93	244	1131.23	+0.59	1126.35	-1.52

TABLE VII

DEGENERATE PAIRS, 110 DRIVEN MODE

RUN#	$f_{(110)}$	Q_1	$f_{(220)}$	FP	$f_{(410)}$	FP
15	1263.38 Hz	315	2527.79 Hz	+0.13	2534.05 Hz	+1.82
16	1265.98	315	2532.95	+0.13	2539.20	+1.81
18	1267.64	307	2536.31	+0.16	2543.54	+2.01

VI. CONCLUSIONS

The experimental system used in testing the theory of Coppens and Sanders has proven to be accurate, efficient, and very reliable. System limitations are few; however, possible equipment improvements are outlined in Appendix B. The system is easily adaptable to cavities or tubes of almost any shape.

It is significant to note that there were no observable differences between the theory of Coppens and Sanders as modified to include empirical losses, for either degenerate or non-degenerate configurations. The theory successfully predicts the basic harmonic content for finite-amplitude standing in a non-perfect rectangular rigid-walled cavity when the piston and its port are relatively small perturbations in the cavity's geometry, regardless of the existences of degeneracies.

The only deviation between theory and experiment can be seen best in Figures 5, 6 and 10. The predicted harmonic distortion for the third harmonic in these cases shows an apparent yielding of power to the fourth harmonic as strength parameter is increased. The experimental data do not conform this feature. It is unclear as to the reason for this discrepancy, but appears to be an artifact brought about by the way the computer program produces E(n) for n's greater than those actually measured. The program presently

calculates values for E(n) not empirically determined, and assigns them alternating positive and negative values of magnitudes consonant to those actually measured. In all cases investigated, the experimental values for E(n) were positive and of order 10^{-4} for the one dimensional cases in question. It is probable that a slight change in the method of calculating higher order values of E(n) could alleviate this lack of agreement. A quick computer run was made using the values obtained for run number 4, and a fabricated value of E(5) which was positive and had a magnitude equal to the average of E(2), E(3), and E(4), and it was found the flattening in the predicted values vanished and more closely resembled the experimental data.

APPENDIX A

INVESTIGATION OF TRAPEZOIDAL CAVITY

One feature incorporated into the design of the rectangular cavity was the ability to turn the adjustable wall around. The side of the wall that was out when in the rectangular configuration, was milled on an angle that had 0.122 in. rise over the 12.002 in length (Figure A1). The mean interior width was adjustable from approximately 5.50 in. to 7.00 in. in 0.25 in. increments. One configuration was investigated in the same manner as were the rectangular ones; a mean width of 5.740 in. was utilized.

The cavity resonances were found to correspond closely to the theoretically predicted frequencies for an ideal rectangular cavity with an interior width dimension of 5.75 in, but always were displaced toward higher frequencies. The cavity was excited at its lowest resonance frequency and the harmonic content recorded. Table A-1 lists the strength parameters, center frequencies, Q(n)'s and E(n)'s measured in this configuration. It is interesting to note that these Q(n)'s were generally lower than those found for configuration A (Table II).

Theoretically predicted curves were generated using the values in Table A-1, and compared to the observed harmonic content (Figures A2-A4). It is clear that there is

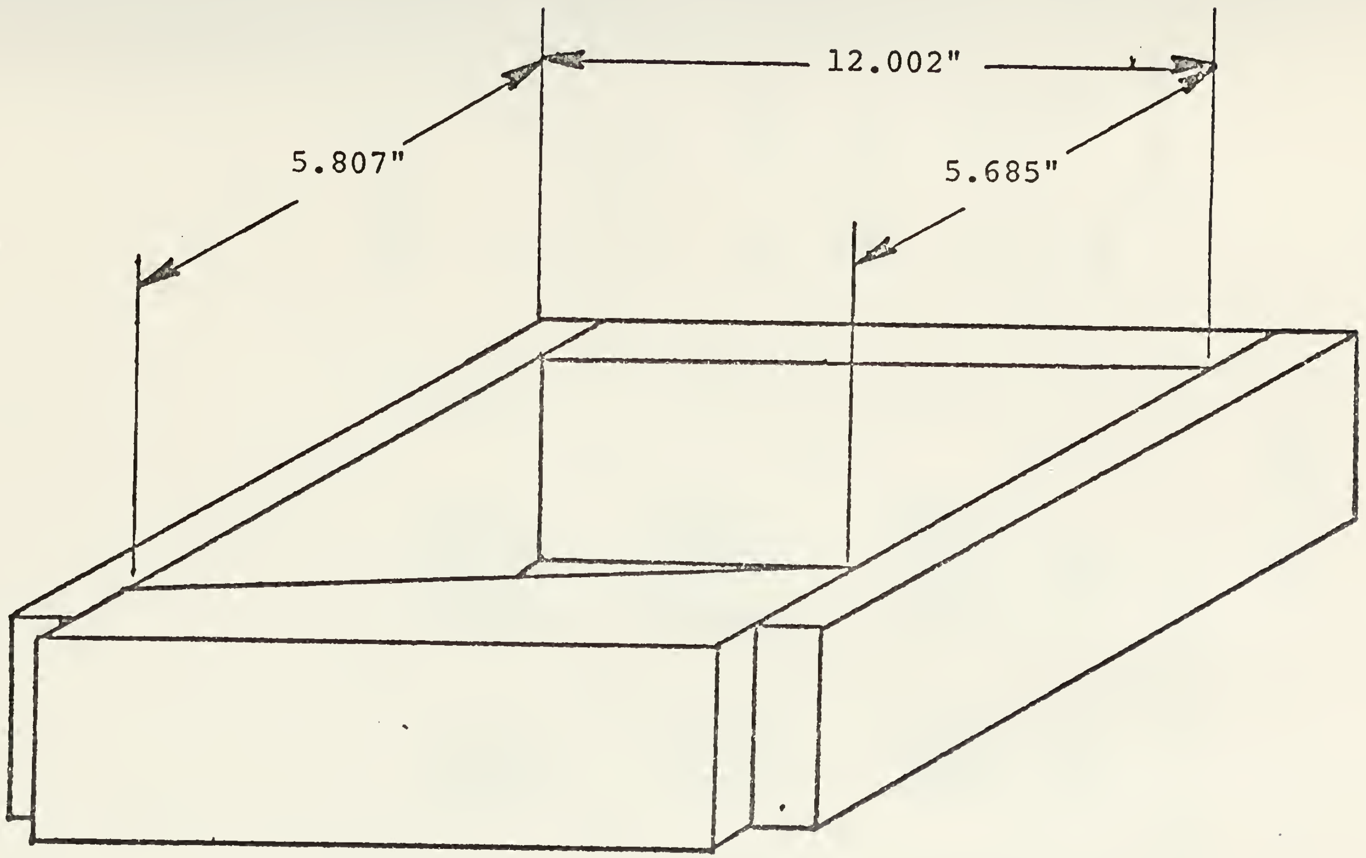

FIGURE A1. TRAPEZOIDAL CAVITY

TABLE A-1

n00 MODES TRAPEZOIDAL CONFIGURATION

SP	RUN#	n	f_{0n} (Hz)	Δf (Hz)	Q(n)	E(n) ($\times 10^3$)
0.269	21	1	565.67	2.40	235	0.0
		2	1132.01	3.18	355	0.684
		3	1698.09	3.84	422	0.636
		4	2264.69	4.64	488	0.886
(fig.A2)						
0.456	20	1	565.51	2.36	239	0.0
		2	1131.75	3.14	360	0.642
		3	1697.68	4.01	423	0.677
		4	2264.24	4.61	491	0.969
(fig.A3)						
0.549	19	1	565.35	2.36	240	0.0
		2	1131.47	3.15	359	0.681
		3	1697.27	4.05	419	0.716
		4	2263.72	4.64	488	1.02
(fig.A4)						

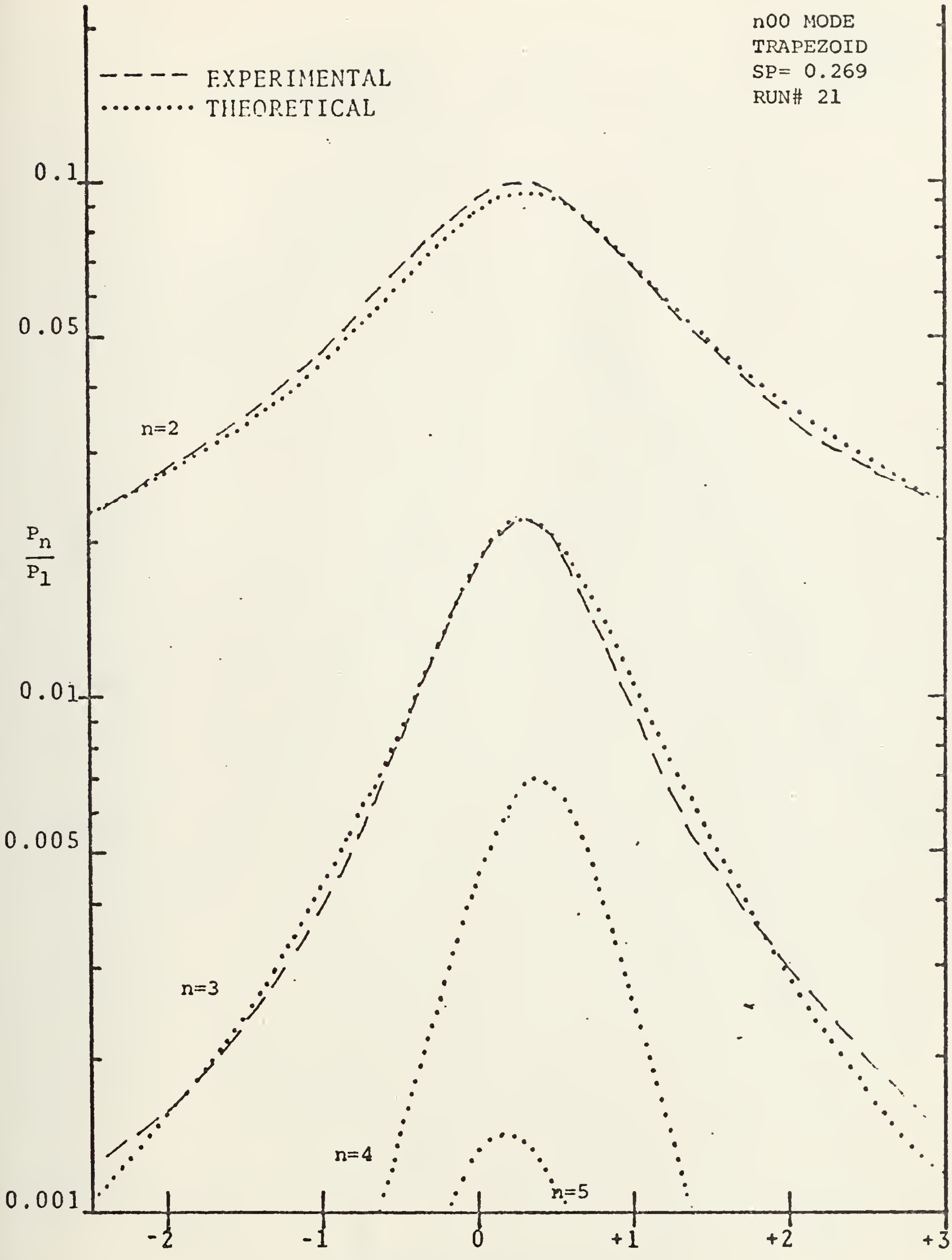
n00 MODE
TRAPEZOID
SP= 0.269
RUN# 21
EXPERIMENTAL
THEORETICAL
0.1
0.05
0.01
0.005
0.001
$\frac{P_n}{P_1}$
n=2
n=3
n=4
n=5
-2
-1
0
+1
+2
+3
FREQUENCY PARAMETER (FP)

FIGURE A2.

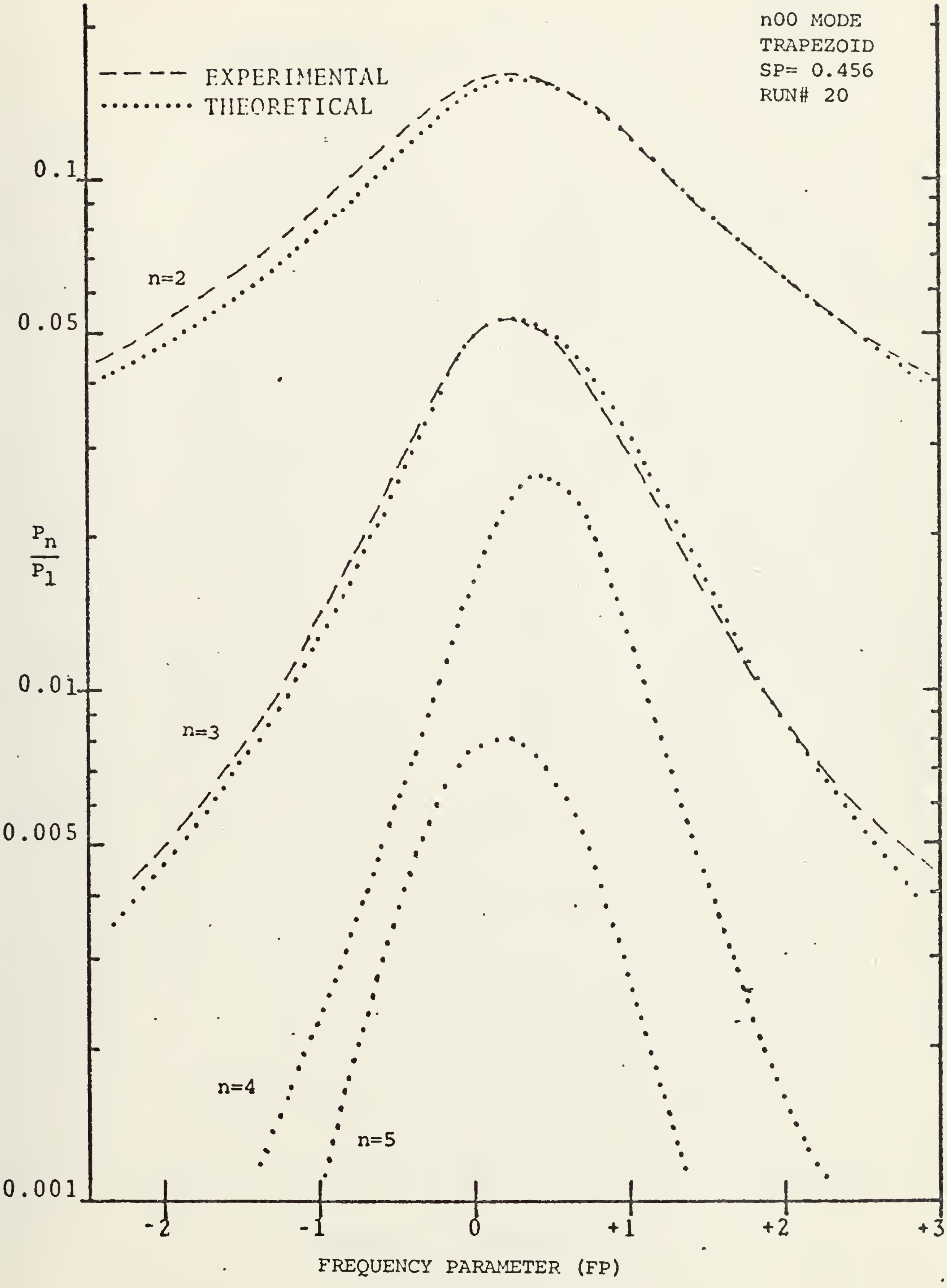

EXPERIMENTAL
THEORETICAL
n00 MODE
TRAPEZOID
SP= 0.456
RUN# 20
0.1
0.05
0.01
0.005
0.001
$\frac{P_n}{P_1}$
n=2
n=3
n=4
n=5
-2
-1
0
+1
+2
+3
FREQUENCY PARAMETER (FP)

FIGURE A3.

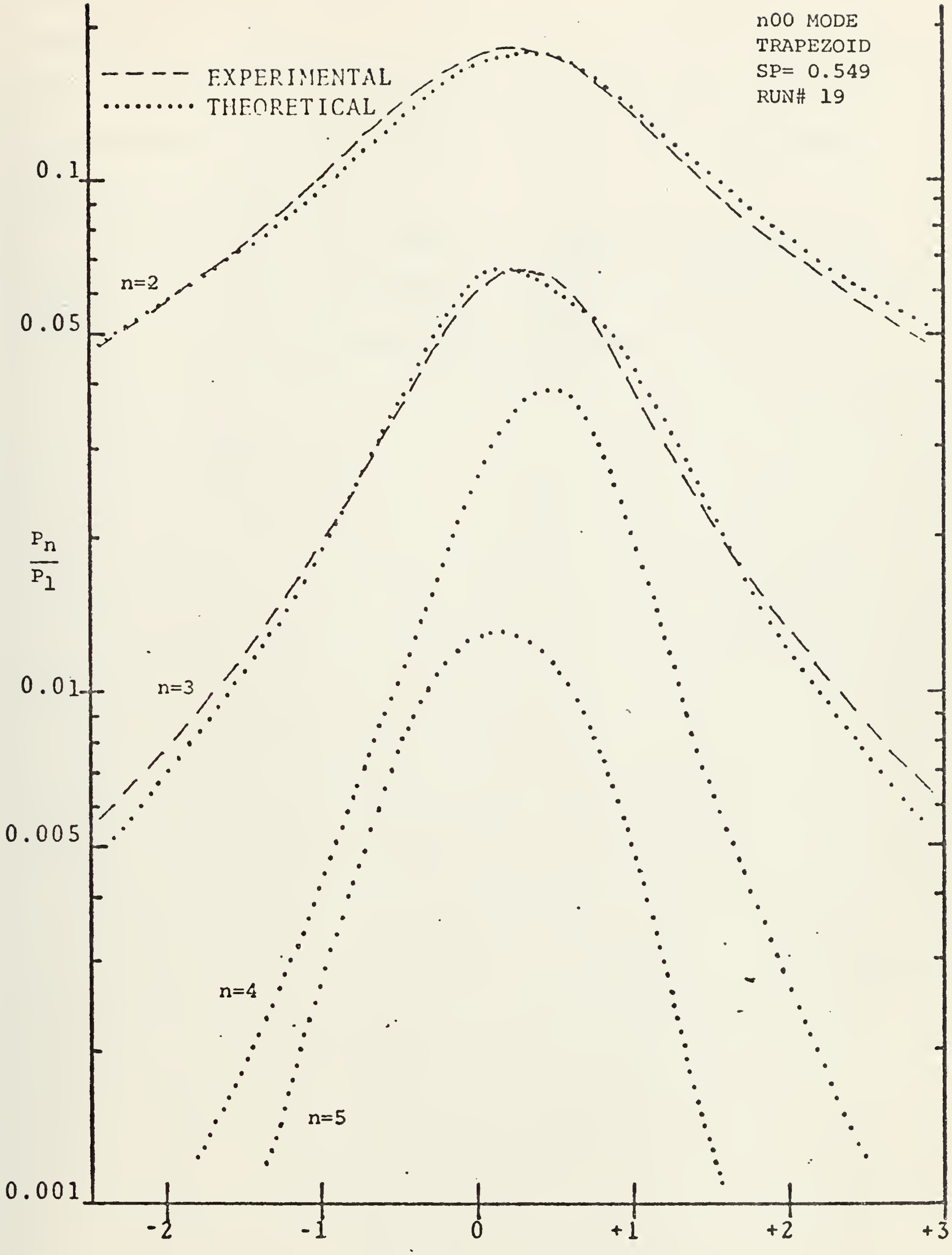

EXPERIMENTAL
THEORETICAL
n00 MODE
TRAPEZOID
SP= 0.549
RUN# 19
0.1
0.05
0.01
0.005
0.001
$\frac{P_n}{P_1}$
n=2
n=3
n=4
n=5
-2
-1
0
+1
+2
+3
FREQUENCY PARAMETER (FP)

FIGURE A4.

excellent agreement in all three runs. The same phenomena exhibited in Figures 5, 6, 10, and 11 is seen in Figure A4, and is believed to be an artifact of the computer's method of calculating values of $E(_n)$ of higher order than those empirically determined.

It appears that the theory of Coppens and Sanders can successfully predict harmonic content for cavities slightly perturbed from rectangular configurations.

APPENDIX B

SUGGESTIONS

The major limitation encountered in this research was the inability to record more than 2 harmonics at one time. What is needed is a six- to eight-track recorder and at least two additional Hewlett Packard HP302A Wave Analyzers. All harmonics to be investigated must be recorded simultaneously to keep any frequency drift from becoming a factor in these measurements.

The General Radio Sweep and Marker Generator model 1160P2 was borrowed from a separate activity. Use of this piece of equipment is essential to the operation of this system.

The final suggestion, but of no less importance, is the necessity of the 0.00 through 0.09 Hz digital component for the existing General Radio model 1161-A Coherent Decade Frequency Synthesizer. The accuracy to which the Sweep Generator's center marker is located is dependent on the Synthesizer's digital components. This final component would eliminate any marker ambiguity that is introduced in the system's present configuration.

BIBLIOGRAPHY

1. Coppens, A. B., and Sanders, J. V., "Finite-Amplitude Standing Waves in Rigid Walled Tubes," J. Acoust. Soc. Am., v. 43, p.516-529, March 1968.

2. Coppens, A. B., and Sanders, J.V., "Finite-Amplitude Waves in Real Cavities," to be published in J. Acoust. Soc. Am., December 1975.

3. Lane, C., Finite-Amplitude Waves in a Rigid Walled Cavity, Thesis, Naval Postgraduate School, Monterey, California, 1972.

4. Devall, R. R., Finite-Amplitude Waves in Imperfect Cavities, Thesis, Naval Postgraduate School, Monterey, California, 1973.

5. Kirchoff, G., Ann. Phys. Leipzig, v. 134, p.177-193, 1868.

6. Lamb, H., Dynamical Theory of Sound, 2d ed., Chap VI, Edward Arnold and Co., London, England, 1925.

7. Fay, R. D., "Plane Sound Waves of Finite Amplitude," J. Acoust. Soc. Am., v. 3, p.222-241, 1931.

8. Fay, R. D., "Successful Method of Attack on Progressive Finite Waves," J. Acoust. Soc. Am., v. 28, p.910-914, September 1956.

9. Keller, J. B., "Finite Amplitude Sound Produced by a Piston in a Closed Tube," J. Acoust. Soc. Am., v. 26, p.253-254, 1954.

10. Keck, W., and Beyer, R. T., "Frequency Spectrum of Finite Amplitude Ultrasonic Waves in Liquids," Phys. Fluids, v. 3, p.346-352, 1960.

11. Weston, D. E., Proc. Phys. Soc., (London) B66, 695-709, 1953.

12. Beech, W. L., Finite-Amplitude Standing Waves in Rigid-Walled Tubes, Thesis, Naval Postgraduate School, Monterey, California, 1967.

13. Ruff, P. G., Finite Amplitude Standing Waves in Rigid Walled Cavities, Thesis, Naval Postgraduate School, Monterey, California, 1967.

14. Winn, J. R., Fourier Analysis of Experimental Finite-Amplitude Standing Waves, Thesis, Naval Postgraduate School, Monterey, California, 1971.

INITIAL DISTRIBUTION LIST

		No. Copies
1.	Defense Documentation Center Cameron Station Alexandria, Virginia 22314	2
2.	Library, Code 0212 Naval Postgraduate School Monterey, California 93940	2
3.	Assoc. Professor James V. Sanders, Code 61Sd Department of Physics and Chemistry Naval Postgraduate School Monterey, California 93940	1
4.	Assoc. Professor Alan B. Coppens, Code 61Cz Department of Physics and Chemistry Naval Postgraduate School Monterey, California 93940	1
5.	LT. Winfield S. Slocum IV, USN 1706 Nimitz Drive Annapolis, Maryland 21401	2
6.	LT. Milo J. Kilmer, USN Service Warfare Officer's School Command Department Head Course Class 51 Newport, Rhode Island 02840	1
7.	Dr. D. T. Blackstock Applied Research Laboratories University of Texas Austin, Texas 78712	1
8.	Department Library, Code 61 Department of Physics and Chemistry Naval Postgraduate School Monterey, California 93940	2

Thesis 163575
S5715 Slocum
c.1 Finite-amplitude standing waves in real cavities containing degenerate modes.